# STING mediates immune responses in the closest living relatives of animals

Arielle Woznica[1*], Ashwani Kumar[2], Carolyn R. Sturge[1], Chao Xing[2], Nicole King[3], Julie K. Pfeiffer[1*]

[1] Department of Microbiology, University of Texas Southwestern Medical Center, Dallas TX 75390, USA
[2] McDermott Center Bioinformatics Lab, University of Texas Southwestern Medical Center, Dallas TX, USA
[3] Howard Hughes Medical Institute, and Department of Molecular and Cell Biology, University of California, Berkeley, Berkeley, CA 94720, USA.

*Correspondence: Arielle.Woznica@UTSouthwestern.edu and Julie.Pfeiffer@UTSouthwestern.edu

## Abstract

Animals have evolved unique repertoires of innate immune genes and pathways that provide their first line of defense against pathogens. To reconstruct the ancestry of animal innate immunity, we have developed the choanoflagellate *Monosiga brevicollis*, one of the closest living relatives of animals, as a model for studying mechanisms underlying pathogen recognition and immune response. We found that *M. brevicollis* is killed by exposure to *Pseudomonas aeruginosa* bacteria. Moreover, *M. brevicollis* expresses STING, which, in animals, activates innate immune pathways in response to cyclic dinucleotides during pathogen sensing. *M. brevicollis* STING increases the susceptibility of *M. brevicollis* to *P. aeruginosa*-induced cell death and is required for responding to the cyclic dinucleotide 2'3' cGAMP. Furthermore, similar to animals, autophagic signaling in *M. brevicollis* is induced by 2'3' cGAMP in a STING-dependent manner. This study provides evidence for a pre-animal role for STING in antibacterial immunity and establishes *M. brevicollis* as a model system for the study of immune responses.

## Introduction

Innate immunity is the first line of defense against pathogens for all animals, in which it is crucial for distinguishing between self and non-self, recognizing and responding to pathogens, and repairing cellular damage. Some mechanisms of animal immunity have likely been present since the last common eukaryotic ancestor, including RNAi, production of antimicrobial peptides, and the production of nitric oxide[1,2]. However, many gene families that play critical roles in animal innate immune responses are unique to animals[3].

Comparing animals with their closest relatives, the choanoflagellates, can provide unique insights into the ancestry of animal immunity and reveal other key features of the first animal, the 'Urmetazoan'[4–6]. Choanoflagellates are microbial eukaryotes that live in diverse aquatic environments and survive by capturing and phagocytosing environmental bacteria[7] using their "collar complex," an apical flagellum surrounded by actin-filled microvilli (Figure 1A)[7,8]. Several innate immune pathway genes once considered to be animal-specific are present in choanoflagellates, including cGAS and STING, both of which are crucial for innate responses to cytosolic DNA in animals (Figure 1- Supplement 1)[3,9,10]. Although the phylogenetic distribution of these gene families reveals that they first evolved before animal origins, their functions in choanoflagellates and their contributions to the early evolution of animal innate immunity are unknown.

STING (stimulator of interferon genes) is a signaling protein that activates innate immune responses to cytosolic DNA during bacterial or viral infection[11,12]. Although STING homologs are conserved in diverse invertebrate and vertebrate animals (reviewed in Margolis et al. 2017)[9,13,14], mechanisms of STING activation are best understood in mammals. In mammals, STING is activated by binding 2'3' cGAMP, an endogenous cyclic dinucleotide produced by the sensor cGAS (cyclic GMP-AMP synthase) upon detecting cytosolic DNA[15–20.]. In addition, cyclic dinucleotides produced by bacteria can also activate STING[17,21]. Importantly, STING domain-containing systems are present in bacteria where they may contribute to anti-phage defense[22,23], raising the possibility that eukaryotic STING-like proteins were acquired from lateral gene transfer[24]. Comparative genomics suggests that STING domains arose at least three independent times in eukaryotes, including once in the stem lineage leading to Choanozoa, the clade containing animals and choanoflagellates[24].

Choanoflagellates have already served as powerful models for studying the origin of animal multicellularity and cell differentiation[10,25–30] and are ideally positioned to yield insights into the evolution of animal immune pathways. Therefore, we sought to establish the choanoflagellate *Monosiga brevicollis* as a model for studying pathogen recognition and immune responses. Here, we report that *Pseudomonas aeruginosa* bacteria are pathogenic for *M. brevicollis.* Through our study of interactions between *P.*

*aeruginosa* and *M. brevicollis*, we determined that STING functions in the choanoflagellate antibacterial response. In addition, we demonstrate that STING is necessary for mediating responses to the STING agonist 2'3' cGAMP *in vivo*, and that 2'3' cGAMP induces STING-dependent autophagic signaling. Our results demonstrate that key features of STING-mediated immune responses are conserved in *M. brevicollis*, thereby expanding our understanding of the pre-metazoan ancestry of STING signaling.

## Results

### *P. aeruginosa* has pathogenic effects on *M. brevicollis*

One impediment to studying immune responses in choanoflagellates has been the lack of known choanoflagellate pathogens. While bacteria are obligate prey and can regulate mating, multicellular development, and cell contractility in choanoflagellates, to our knowledge no bacteria with pathogenic effects have been described [25,28,29,31–33]. For this study, we focused on the choanoflagellate *Monosiga brevicollis,* which has a sequenced genome[4] and grows robustly under laboratory conditions in co-culture with *Flavobacterium* prey bacteria[5]. To identify potential pathogens of choanoflagellates, we screened select bacteria – including environmental isolates and known animal pathogens and commensals (Table 1) – to test whether any of these induced *M. brevicollis* behavioral changes or reduced cell survival.

After co-culturing *M. brevicollis* with bacteria for 24 hours, only the gammaproteobacterium *Pseudomonas aeruginosa,* a ubiquitous environmental bacterium and opportunistic pathogen of diverse eukaryotes[34–37], altered the behavior and growth dynamics of *M. brevicollis*. Under standard laboratory conditions, *M. brevicollis* is a highly motile flagellate and swims up in the water column (Video 1, Supplementary file 1). However, after 12-14 hours in the presence of *P. aeruginosa* strains PAO1 and PA14, a large proportion of *M. brevicollis* cells settled to the bottom of the culture dish (Video 1, Supplementary file 1 ). Immunofluorescence staining revealed that *M. brevicollis* cells exposed to *P. aeruginosa* had truncated flagella compared to cells exposed to *E. coli* or other bacteria that did not induce cell settling (Figure 1B). To determine the effects of *P. aeruginosa* on cell viability, we added *P. aeruginosa* strain PAO1 or control gammaproteobacteria to *M. brevicollis* and monitored cell density over the course of 72 hours (Figure 1C). While *M. brevicollis* continued to proliferate in the presence of control gammaproteobacteria, exposure to *P. aeruginosa* PAO1 resulted in cell death.

Choanoflagellates prey upon bacteria and ingest them through phagocytosis[7,8]. However, many bacterial pathogens, including *P. aeruginosa*, have evolved strategies to prevent or resist phagocytosis by eukaryotic cells[38,39]. Therefore, we examined

121 whether phagocytosis of *P. aeruginosa* is required to induce cell death. To track
122 phagocytosis, we added GFP-expressing *E. coli* DH5α (Figure 1D) or *P. aeruginosa*
123 PAO1 (Figure 1E) to *M. brevicollis* and monitored the cultures by live imaging. After one
124 hour, while 92% of *M. brevicollis* cells incubated with *E. coli*–GFP had GFP+ food
125 vacuoles, only 3% of cells incubated with PAO1-GFP had GFP+ food vacuoles (Figure
126 1F). *M. brevicollis* also robustly phagocytosed GFP-expressing *V. parahaemolyticus*
127 and *C. jejuni* (Figure 1F).
128 Next, to determine if *P. aeruginosa* broadly disrupts *M. brevicollis* phagocytosis,
129 which could induce cell death through starvation, we incubated *M. brevicollis* with GFP-
130 expressing PAO1 or GFP-expressing *E. coli* for one hour, and then added 0.2 mm
131 fluorescent beads for an additional 30 minutes as an independent measure of
132 phagocytic activity. The fraction of *M. brevicollis* cells with internalized 0.2 mm beads
133 was similar in cultures incubated with *E. coli* DH5α and PAO1 (Figure 1G). Moreover,
134 exposure to *P. aeruginosa* did not inhibit phagocytic uptake of *E. coli* (Figure 1H). These
135 results suggest that exposure to *P. aeruginosa* does not broadly inhibit phagocytosis.
136 The above results suggested that the pathogenic effects of *P. aeruginosa* are
137 induced by factors secreted by extracellular bacteria. In addition, diverse secreted
138 bacterial molecules have been previously shown to influence choanoflagellate cell
139 biology[25,28,31]. Therefore, we next investigated the effects of secreted *P. aeruginosa*
140 molecules on *M. brevicollis* viability. Exposure of *M. brevicollis* to conditioned medium
141 from *P. aeruginosa* PAO1 or diverse non-pathogenic gammaproteobacteria revealed
142 that PAO1 conditioned medium is sufficient to restrict growth and induce cell death
143 (Figure 1I). Similar to live bacteria, exposure to *P. aeruginosa* conditioned medium led
144 to reduced motility and truncated flagella in *M. brevicollis* after approximately 8-10
145 hours.
146 Because numerous *P. aeruginosa* secreted virulence factors have been
147 characterized[34,40], we screened a battery of isogenic PAO1 strains with deletions in
148 known virulence genes to determine if any of these factors contribute to the pathogenic
149 effects on *M. brevicollis* (Table 2). All strains tested induced similar levels of *M.*
150 *brevicollis* cell death as the parental PAO1 strain, suggesting that none of the deleted
151 virulence genes alone are essential for inducing cytotoxicity in *M. brevicollis*. The
152 bioactivity in the conditioned media was also found to be heat, protease, and nuclease
153 resistant, indicating that the virulence factors are unlikely to be proteins or nucleic acids
154 (Table 3). In addition, we found that subjecting the conditioned media to methanol
155 extraction followed by liquid chromatography-mass spectrometry resulted in specific
156 fractions that recapitulated the bioactivity of the conditioned media. Although further
157 detailed chemical analysis is required to determine the molecular nature of these
158 factors, these data indicate that secreted *P. aeruginosa* small molecules are sufficient
159 for inducing cell death in *M. brevicollis.*

Finally, we investigated whether transient exposure to *P. aeruginosa* is sufficient to induce cell death in *M. brevicollis* (Figure 1J). Because choanoflagellates likely experience fluctuations in the chemical composition of aquatic microenvironments on various timescales, we exposed stationary-phase *M. brevicollis* to *P. aeruginosa* conditioned media for increasing durations, and then assessed survival relative to *Flavobacterium*-treated controls after 24 hours. While *M. brevicollis* cell death was not observed after treatment with *P. aeruginosa* conditioned media for 4 hours or less, exposures lasting for 6 hours or longer reduced *M. brevicollis* survival (Figure 1J). These results suggest that cell death pathways are not induced immediately in response *P. aeruginosa* virulence factors, but are activated after longer exposures to *P. aeruginosa.*

**Upregulation of *M. brevicollis* STING in response to *P. aeruginosa***

To identify potential genetic pathways activated by *M. brevicollis* in response to pathogenic bacteria*,* we performed RNA-seq on *M. brevicollis* exposed to conditioned medium from either *P. aeruginosa* or *Flavobacterium sp*., the non-pathogenic bacterial strain used as a food source (Table 1). We found that 674 genes were up-regulated and 232 genes were downregulated two-fold or greater (FDR≤$10^{-4}$) upon *P. aeruginosa* exposure compared to cells exposed to *Flavobacterium* (Figure 2A). The up-regulated genes were enriched in biological processes including response to stress, endocytosis, microtubule-based movement, mitochondrial fission, and carbohydrate metabolism. Genes down-regulated in response to *P. aeruginosa* were enriched in biological processes including RNA modification and metabolism (Figure 2 - figure supplement 1A). We also found that the transcription of several genes encoding proteins that function in animal antibacterial innate immunity was upregulated in response to *P. aeruginosa*, including C-type lectin, glutathione peroxidase, and STING (Figure 2A,B). Using an antibody we raised against the C-terminal portion of *M. brevicollis* STING (Figure 2 - figure supplement 1C) we found that STING protein levels are also elevated in response to *P. aeruginosa* (Figure 2C). Given the importance of STING in animal immunity and its upregulation in response to *P. aeruginosa*, we pursued its functional relevance in the *M. brevicollis* pathogen response.

**The cyclic dinucleotide 2'3' cGAMP induces elevated expression of STING in *M. brevicollis***

The predicted domain architecture of *M. brevicollis* STING consists of four transmembrane domains followed by a cytosolic STING domain (Fig. 3A, Figure 2 - figure supplement 1D), and likely matches the structure of the ancestral animal STING protein. Vertebrate STING proteins contain a C-terminal tail (CTT; Fig. 3A, Figure 2 -

figure supplement 1D) that is required for the induction of interferons[41–43], and for the activation of other downstream responses, including NFkB[44] and autophagy[45–47] pathways. Both the STING CTT and interferons evolved in vertebrates, and it is currently unclear how choanoflagellate and invertebrate STING proteins mediate downstream immune responses[13,48]. However, the conservation of putative cyclic dinucleotide-binding residues in *M. brevicollis* STING (Fig. 3B) led us to hypothesize that STING signaling may be induced by cyclic dinucleotides. In addition, because *M. brevicollis* has a cGAS-like enzyme (Figure 1- Supplement 1A), it is possible that *M. brevicollis* produces an endogenous cyclic dinucleotide similar to mammalian 2'3' cGAMP[9,12,49].

To identify potential STING inducers[49,50], we treated *M. brevicollis* with purified cyclic dinucleotides, including mammalian cGAMP (2'3' cGAMP) and bacterial cyclic dinucleotides (3'3' c-di-GMP, 3'3' c-di-AMP, 3'3' cGAMP). We first performed dose-response curves to determine if the different cyclic dinucleotides affect the viability of *M. brevicollis* (Fig. 3C). Interestingly, we found that exposure to 2'3' cGAMP induced cell death in a dose-dependent manner. In contrast, exposure to 3'3' cGAMP, c-di-GMP, and c-di-AMP did not alter *M. brevicollis* survival. Transcriptional profiling of *M. brevicollis* revealed a robust transcriptional response to 2'3' cGAMP after three hours (Figure 3 - figure supplement 1A). Moreover, transcriptional profiling of *M. brevicollis* exposed to 2'3' cGAMP or 3'3' cGAMP for three hours revealed that *STING* mRNA levels increase in response to 2'3' cGAMP, but remain unchanged in response to 3'3 cGAMP (Figure 3 - figure supplement 1A-C). Therefore, we next treated *M. brevicollis* with the cyclic dinucleotides for five hours, and measured STING protein levels by immunoblot (Fig. 3D). Treatment with 2'3' cGAMP, but not the bacterially-produced cyclic dinucleotides, led to elevated levels of STING protein compared to unstimulated cells. A time course of 2'3' cGAMP treatment revealed that STING protein levels increase as early as three hours after exposure to the cyclic dinucleotide and remain elevated for at least 7 hours, approximately one cell cycle (Fig. 3E). While we also observed sustained upregulation of STING in the presence of *P. aeruginosa*, this is markedly different from what has been described in mammals, wherein STING activation results in its translocation to lysosomes and degradation[47]. In addition, immunostaining for STING in fixed *M. brevicollis* revealed that the number and intensity of STING puncta increases after exposure to 2'3' cGAMP (Figure 3 - figure supplement 1E,F), although the localization of STING was difficult to assess by immunostaining due to a lack of available subcellular markers. These data suggest that *M. brevicollis* STING responds to 2'3' cGAMP, and that this cyclic dinucleotide can be used to further characterize the role of STING in *M. brevicollis*.

**Transfection reveals that STING localizes to the *M. brevicollis* endoplasmic reticulum**

240
241 A key barrier to investigating gene function in *M. brevicollis* has been the
242 absence of transfection and reverse genetics. We found that the transfection protocol
243 recently developed for the choanoflagellate *Salpingoeca rosetta*[50] was not effective in
244 *M. brevicollis*, but by implementing a number of alterations to optimize reagents and
245 conditions (see Methods) we were able to achieve both reproducible transfection and
246 establishment of stably transformed cell lines in *M. brevicollis*.
247 To investigate the subcellular localization of STING, we established a robust
248 transfection protocol for *M. brevicollis* that would allow the expression of fluorescently-
249 labeled STING along with fluorescent subcellular markers for different organelles.
250 We observed that STING-mTFP protein localized to tubule-like structures around the
251 nucleus (Figure 5A) similar to what was observed by immunostaining with an antibody
252 to STING (Figure 3 - figure supplement 1E,F). We then co-transfected STING-mTFP
253 alongside fluorescent reporters marking the endoplasmic reticulum (ER) or mitochondria
254 (Figure 5B,C) and performed live-cell imaging. STING-mTFP co-localized with a
255 fluorescent marker highlighting the ER (Figure 5B). Thus, as in mammalian cells[15,51],
256 STING localizes to regions of the ER in *M. brevicollis*.
257
258 **Genetic disruption of STING reveals its role in responding to 2'3' cGAMP and *P.***
259 ***aeruginosa***
260
261 Disrupting the *STING* locus using CRISPR/Cas9-mediated genome editing
262 (Figure 5A) enabled us to investigate the function of STING. To overcome low gene
263 editing efficiencies in *M. brevicollis,* we based our gene editing strategy on a protocol
264 recently developed for *S. rosetta* that simultaneously edits a gene of interest and
265 confers cycloheximide resistance[52]. By selecting for cycloheximide resistance and then
266 performing clonal isolation, we were able to isolate a clonal cell line that has a deletion
267 within the *STING* locus that introduces premature stop codons (Figure 5 - figure
268 supplement 1A). We were unable to detect STING protein in *STING*$^{-}$ cells by
269 immunoblot (Figure 5B). Wild type and *STING*$^{-}$ cells have similar growth kinetics (Figure
270 5 - figure supplement 1B), suggesting that STING is not required for cell viability under
271 standard laboratory conditions. In addition, overexpression of STING-mTFP did not
272 affect *M. brevicollis* viability.
273 To investigate the connection between 2'3' cGAMP and STING signaling in *M.*
274 *brevicollis*, we exposed *STING*$^{-}$ cells to increasing concentrations of 2'3' cGAMP. In
275 contrast to wild type *M. brevicollis*, *STING*$^{-}$ cells are resistant to 2'3' cGAMP-induced
276 cell death (Figure 5C). The 2'3' cGAMP resistance phenotype could be partially
277 reversed by stably expressing STING within the *STING*$^{-}$ mutant background (Figure
278 5D). In addition, *STING*$^{-}$ cells fail to induce a strong transcriptional response to 2'3'
279 cGAMP compared to wild type cells (Figure 5E, Figure 3 - figure supplement 1A, Figure

5 - figure supplement 1C,D). While 371 genes are differentially expressed in wild type cells after exposure to 2'3' cGAMP for three hours, only 28 genes are differentially expressed in *STING*$^{-}$ cells (FC ≥3; FDR≤$10^{-4}$). Thus, 2'3' cGAMP induces a STING-dependent transcriptional response in *M. brevicollis*.

Interestingly, of the 22 choanoflagellate species with sequenced transcriptomes[3,29], only *M. brevicollis* and *Salpingoeca macrocollata*, express homologs of both STING and cGAS (Figure 1- Supplement 1A, Figure 5F, Figure 5 - figure supplement 1E). Therefore, we were curious whether other choanoflagellate species are able to respond to 2'3' cGAMP in the absence of a putative STING protein. We exposed four other choanoflagellate species (*Salpingoeca infusionum*, *S. macrocollata, S. rosetta*, and *Salpingoeca punica*) to increasing 2'3' cGAMP concentrations, and quantified survival after 24 hours (Figure 5G). Of these additional species, only *S. macrocollata* had impaired survival in the presence of 2'3' cGAMP. Thus, it is possible that STING also responds to 2'3' cGAMP in *S. macrocollata.*

We next asked whether *STING*$^{-}$ cells have altered responses to other immune agonists. Although *M. brevicollis* is continuously co-cultured with feeding bacteria, we observed that treatment with high concentrations of *E. coli* lipopolysaccharides induces cell death (Figure 5H). As LPS is not known to activate STING signaling, we treated wild type and *STING*$^{-}$ cells with LPS to probe the specificity of STING-mediated immune responses in *M. brevicollis*. The survival responses of wild type and *STING*$^{-}$ cells to LPS were indistinguishable (Figure 5H), suggesting that there are separable pathways for responding to 2'3' cGAMP and LPS. We also examined the survival of *STING*$^{-}$ cells exposed to *P. aeruginosa* conditioned medium (Figure 5I,J). In growth curve experiments, *P. aeruginosa* hindered the growth rate and stationary phase cell density of *STING*$^{-}$ cells compared to *Flavobacterium* (Figure 5I,J). However, *STING*$^{-}$ cells were still able to divide in the presence of *P. aeruginosa,* whereas wild type cell growth was completely restricted (Figure 5I,J). These results indicate that wild type cells are more susceptible to *P. aeruginosa* than *STING*$^{-}$ cells, although it is unclear how STING contributes to *P. aeruginosa*-induced growth restriction and cell death.

**2'3' cGAMP-induces autophagic signaling via STING**

One downstream consequence of STING signaling in animals is the initiation of autophagy[21,45,46,49,53]. Based on viral infection studies in *D. melanogaster*[53] and experiments expressing invertebrate STING in mammalian cells[45], it has been proposed that the induction of autophagy may be an interferon-independent ancestral function of STING. Although *M. brevicollis* lacks many effectors required for immune responses downstream of STING in animals (including TBK1 and NF-kB; Figure S1A),

319 autophagy machinery is well conserved in *M. brevicollis*. Therefore, we asked if one
320 outcome of 2'3' cGAMP exposure in *M. brevicollis* is the induction of autophagy.
321 The evolutionarily conserved protein Atg8/LC3 is a ubiquitin-like protein that can
322 be used to monitor autophagy[54,55]. During autophagosome formation, unmodified Atg8,
323 called Atg8-I, is conjugated to phosphatidylethanolamine. Lipidated Atg8, called Atg8-II,
324 remains associated with growing autophagosomes. As such, two indicators of
325 autophagy are elevated Atg8-II levels relative to Atg8-I and increased formation of
326 Atg8+ autophagosome puncta. Because antibodies are not available to detect
327 endogenous *M. brevicollis* autophagy markers or cargo receptors, we generated wild
328 type and *STING*$^{-}$ cell lines stably expressing mCherry-Atg8. Stable expression of
329 mCherry-Atg8 under the control of the constitutive pEFL promoter did not alter the
330 relative susceptibilities of these cell lines to 2'3'cGAMP (Figure 6 - figure supplement
331 1A). By immunoblot, mCherry-Atg8-II can be distinguished from mCherry-Atg8-I based
332 on its enhanced gel mobility. When we exposed both cell lines to 2'3' cGAMP for three
333 hours, we observed increased levels of Atg8-II relative to Atg8-I by immunoblot in wild
334 type, but not *STING*$^{-}$ cells (Figure 6A). These results suggest that treatment with 2'3'
335 cGAMP induces autophagic signaling in a STING-dependent manner; however, making
336 this conclusion requires evidence of autophagy induction through inhibitor studies. To
337 confirm autophagy induction, we treated cells with chloroquine, a lysosomotropic agent
338 which inhibits autophagy by blocking endosomal acidification, thereby preventing
339 amphisome formation and Atg8-II turnover[54]. Exposing wild type cells pretreated with
340 chloroquine to 2'3' cGAMP for three hours resulted in increased levels of Atg8-II relative
341 to Atg8-I, suggesting that 2'3' cGAMP treatment indeed induces the autophagic
342 pathway (Figure 6B, Figure 6 - figure supplement 1B). In cells pretreated with
343 chloroquine, STING levels did not markedly increase after exposure to 2'3' cGAMP
344 (Figure 6 - figure supplement 1B), raising the possibility that the autophagic pathway is
345 important for regulating STING protein levels. We next examined whether 2'3' cGAMP
346 induces Atg8+ puncta formation by treating wild type and *STING*$^{-}$ cells with 2'3' cGAMP
347 for three hours, and observing mCherry foci by microscopy (Figure 6C-F). Quantifying
348 images revealed that Atg8+ puncta accumulate after 2'3' cGAMP treatment in wild type,
349 but not *STING*$^{-}$ cells (Figure 6G). Overall, these results suggest that *M. brevicollis*
350 responds to 2'3' cGAMP through STING-dependent induction of the autophagy
351 pathway.
352 Finally, we asked whether STING-mediated autophagic pathway induction affects
353 survival after exposure to 2'3' cGAMP (Figure 6H). To determine if inhibiting autophagy
354 impacts 2'3' cGAMP-induced cell death, we examined the survival responses of wild
355 type and *STING*$^{-}$ *M. brevicollis* to 2'3' cGAMP after pretreatment with lysosomotropic
356 agents chloroquine or $NH_4Cl$. Chloroquine or $NH_4Cl$ pretreatment rescued 2'3' cGAMP-
357 induced cell death in wild type *M. brevicollis* (Figure 6H), whereas the survival of
358 *STING*$^{-}$ cells, which are already resistant to 2'3' cGAMP-induced cell death, was not

359 affected. Therefore, we hypothesize that 2'3' cGAMP induces cell death in *M. brevicollis*
360 by overstimulating STING-mediated autophagic signaling.
361
362 **Discussion**
363
364 Investigating choanoflagellate immune responses has the potential to inform the
365 ancestry of animal immune pathways. In this study, we screened diverse bacteria to
366 identify a choanoflagellate pathogen, and determined that *M. brevicollis* is killed by
367 sustained exposure to *P. aeruginosa* bacteria. We found that STING, a crucial
368 component of animal innate responses to cytosolic DNA, is upregulated in *M. brevicollis*
369 after exposure to *P. aeruginosa* or the STING ligand 2'3' cGAMP. The application of
370 newly-developed transgenic and genetic tools for *M. brevicollis* revealed that, similar to
371 mammalian STING, *M. brevicollis* STING localizes to perinuclear endoplasmic reticulum
372 regions. In addition, STING mediates responses to *P. aeruginosa* bacteria, and is
373 required for inducing transcriptional changes and autophagic signaling in response to
374 2'3' cGAMP. These data reveal that STING plays conserved roles in choanoflagellate
375 immune responses, and provide insight into the evolution of STING signaling on the
376 animal stem lineage.
377 The discovery that *M. brevicollis* STING mediates immune responses raises a
378 number of interesting questions about the full extent of its physiological roles in
379 choanoflagellates. For example, while our results demonstrate that *M. brevicollis* STING
380 responds to exogenous 2'3' cGAMP, the endogenous triggers of STING activation in *M.*
381 *brevicollis* remain to be determined. *M. brevicollis* has a putative cGAS homolog,
382 suggesting that STING may respond to an endogenously produced cyclic dinucleotide
383 similar to 2'3' cGAMP. Determining the enzymatic activities of *M. brevicollis* cGAS and
384 identifying the endogenous trigger of *M. brevicollis* STING will be critical steps towards
385 elucidating mechanisms of STING activation. Although cGAS and STING are rare
386 among sequenced choanoflagellate species, both species with STING homologs, *M.*
387 *brevicollis* and *S. macrocollata*, also harbor a cGAS homolog (Figure 1- Supplement
388 1A), suggesting the presence of an intact choanoflagellate cGAS-STING pathway.
389 Our results suggest that *M. brevicollis* has distinct responses to 2'3' cGAMP
390 versus 3'3'-linked cyclic dinucleotides produced by bacteria (Figure 3C,D, Figure 3 -
391 figure supplement 1). In contrast to 2'3' cGAMP, bacterial cyclic dinucleotides (3'3'
392 cGAMP, c-di-AMP, c-di-GMP) do not induce cell death in *M. brevicollis*. However, 3'3'
393 cGAMP induces a robust transcriptional response in *M. brevicollis,* indicating that
394 STING, or a different cyclic dinucleotide receptor[57], responds to these bacterial
395 molecules. One hypothesis is that *M. brevicollis* STING, similar to animal STING
396 proteins[14], may have different binding affinities for 2'3' and 3'3'-linked cyclic
397 dinucleotides. It is also possible that bacterial cyclic dinucleotides activate additional
398 pathways that influence survival in *M. brevicollis*. As bacterivores, choanoflagellates

399 likely benefit from a fine-tuned response to bacterial cyclic dinucleotides that enables
400 them to interpret higher and lower concentrations in their environment. Elucidating
401 mechanisms of STING activation in *M. brevicollis* could help reveal how STING proteins
402 in animals evolved to respond to both bacterially-produced and endogenous cyclic
403 dinucleotides.
404 While it is clear that 2'3' cGAMP stimulates STING-dependent transcriptional
405 responses and autophagic signaling in *M. brevicollis* (Figure 5, Figure 6), the signaling
406 pathways downstream of STING in choanoflagellates are unknown. Much of what is
407 known about STING signaling comes from mammals and involves the extended CTT
408 domain of STING, which *M. brevicollis* lacks, and immune genes that are restricted to
409 vertebrates. Two pathways downstream of STING activation that are conserved in
410 invertebrates, and as such are proposed ancestral functions of STING, are autophagy
411 and NF-kB signaling. Here, we observed that STING is required for induction of the
412 autophagy pathway in response to 2'3' cGAMP in *M. brevicollis*, indicating that the role
413 of STING in regulating autophagy predates animal origins. While exposure to 2'3'
414 cGAMP leads to NF-kB activation in the sea anemone *N. vectensis*[58] and in insects[59–62],
415 neither *M. brevicollis* nor *S. macrocollata*, the two choanoflagellate species with STING,
416 possess a NF-kB homolog[3]. Nonetheless, 2'3' cGAMP activates an extensive
417 transcriptional response downstream of STING in *M. brevicollis*, although the specific
418 signaling pathways remain to be identified. This does not negate the hypothesis that
419 STING signaling led to NF-kB activation in the Urmetazoan, but strongly suggests that
420 additional pathways exist downstream of STING activation in choanoflagellates, and
421 potentially in animals.
422 Choanoflagellates forage on diverse environmental bacteria for sustenance, yet
423 how they recognize and respond to pathogens is a mystery. Our finding that *P.*
424 *aeruginosa* has pathogenic effects on *M. brevicollis* (Figure 1) provides a much-needed
425 framework for uncovering mechanisms of pathogen recognition and antibacterial
426 immunity in choanoflagellates. Profiling the host transcriptional response to *P.*
427 *aeruginosa* has allowed us to identify choanoflagellate genes that may be involved in
428 recognizing (C-type lectins) and combating (polysaccharide lyases, antimicrobial
429 peptides) bacteria; yet, it has also revealed the immense complexity of this interaction,
430 with more than 600 *M. brevicollis* genes differentially expressed in response *P.*
431 *aeruginosa*. Thus, identifying specific *P. aeruginosa* virulence factors will be critical for
432 understanding why *P. aeruginosa* – but not other bacteria – have pathogenic effects on
433 *M. brevicollis,* and facilitate the characterization of mechanisms underlying
434 choanoflagellate pathogen responses.
435 With the establishment of molecular genetic techniques in choanoflagellates --
436 first for *S. rosetta*[50,52]*,* and here for *M. brevicollis* -- we now have the opportunity to
437 explore the functions of candidate immune genes. Identifying additional
438 choanoflagellate pathogens, particularly viral pathogens, will also be key to delineating

immune response pathways. Finally, as choanoflagellates are at least as genetically diverse as animals[3], expanding studies of immune responses to diverse choanoflagellate species will be essential for reconstructing the evolution of immune pathways in animals.


## Acknowledgements

We thank Bill Jackson, Tera Levin, Shally Margolis, Russell Vance, and Nan Yan for helpful advice and/or comments on the manuscript, and David Greenberg, David Hendrixson, Andrew Koh, Kim Orth, Russell Vance, and Sebastian Winter for bacterial strains. We thank Neal Alto for use of the widefield microscope, Monika Sigg for use of a reporter construct, and Mya Breitbart for sea water samples. We are grateful for David Booth's invaluable advice on developing transfection and gene editing protocols.

This work was funded by a Pew Innovation Fund award (JKP and NK), a HHMI Hanna Gray Fellows award (AW), a HHMI Faculty Scholar award (JKP), and a Burroughs Wellcome Fund Investigators in the Pathogenesis of Infectious Diseases (JKP). We acknowledge the assistance of the UT Southwestern Live Cell Imaging Facility, a Shared Resource of the Harold C. Simmons Cancer Center, supported in part by an NCI Cancer Center Support Grant, 1P30 CA142543-01.


## Materials and Methods

**Key Resources Table**

| **Reagent type (species) or resource** | **Designation** | **Source or reference** | **Identifiers** | **Additional information** |
|---|---|---|---|---|
| Strain, strain background (*M. brevicollis*) | *M. brevicollis* | ATCC PRA-258 | PMID: 18276888 | |
| Genetic reagent, (*M. brevicollis*) | *M. brevicollis STING*$^{-}$ | This study | | *STING*$^{-}$ knockout strain ; cell line maintained |

| | | | | |
|---|---|---|---|---|
| | | | | by A. Woznica |
| Transfected construct (*M. brevicollis*) | pEFL5'-pac-P2A-STING-mTFP-3'act | This study | | Construct to express *M, brevicollis* STING fused to mTFP; can be obtained from A. Woznica |
| Transfected construct (*M. brevicollis*) | pEFL5'-pac-P2A-mCherry-Atg8--3'act | This study | | Construct to express mCherry fused to *M. brevicollis* Atg8; can be obtained from A. Woznica |
| Strain, strain background(*Flavobacterium*) | *Flavobacterium* sp. | This study | | Isolated from MX1 (ATCC PRA-258) culture; can be obtained from A. Woznica |
| Strain, strain background(*Pseudomonas aeruginosa*) | PAO1 | ATCC 15692 | PMID: 13961373 | |
| *P. aeruginosa*, transgenic strain | PAO1-GFP | ATCC 15692GFP | PMID: 9361441 | |
| Antibody | anti-choano STING (rabbit polyclonal) | This study | | Generated by Pacific Immunology; dilution 1:200 for IF, 1:2000 dilution for |

| | | | | |
|---|---|---|---|---|
| | | | | WB; can be obtained from A. Woznica |
| antibody | Anti-mCherry 16D7 (rat monoclonal) | Invitrogen | Cat# M11217 | 1:2000 dilution for WB |
| antibody | Anti-human Tubulin E7 (Mouse monoclonal) | Developmental Studies Hybridoma Bank | Cat# AB_2315513 | 1:200 dilution for IF |
| antibody | Alpha-human tubulin (Mouse monoclonal) | Sigma Aldrich | Cat # T64074 | 1:7000 dilution for WB |
| Chemical compound, drug | 2’3’ cGAMP | Cayman Chemical | Cat# 19887 | |
| Chemical compound, drug | 3’3’ cGAMP | Cayman chemical | Cat# 17966 | |
| Sequence-based reagent | *STING556* gRNA | This study | Guide RNA | TTTCGGGATTCAGATGTGGG |
| Sequenced-based reagent | *STING* locus PCR primers | This study | PCR primers | F: 5’ ATG ATG GTT AAT CTC TCT GAT CTT TCA CAT C 3’ R: 5’ TTA TGG CAT CGC ATA CTG GTC C 3’ |

| | | | | |
|---|---|---|---|---|
| Commercial assay, kit | SG Cell Line 4D-NucleofectorTM X Kit S | Lonza, | Cat# V4XC-3032 | |

464
465
466 Culturing choanoflagellates
467 All strains of *M. brevicollis* were co-cultured with *Flavobacterium sp.* bacteria[4]
468 (American Type Culture Collection [ATCC], Manassas, VA; Cat. No. PRA-258) in a
469 seawater based media enriched with glycerol, yeast extract, peptone and cereal grass
470 (details in Media Recipes). Cells were grown either at room temperature, or at 16ºC in a
471 wine cooler (Koldfront). All *M. brevicollis* cell lines were verified by 18S sequencing and
472 RNA-seq. Choanoflagellate cell lines *S. rosetta*, *S. macrocollata*, *S. punica*, and *S.*
473 *infusionum* were verified by 18S sequencing.
474
475 Bacterial effects on *M. brevicollis*
476 ***Isolating environmental bacteria***
477 Environmental bacterial species were isolated from water samples from Woods
478 Hole, MA, St. Petersburg, FL, and Dallas, TX. Water samples were streaked onto Sea
479 Water Complete media or LB plates, and grown at 30º C or 37º C. After isolating
480 individual colonies, partial 16S sequencing using 16S universal primers (27F: 5′-
481 AGAGTTTGATCCTGGCTCAG-3′, 1492R: 5′-TACGGYTACCTTGTTACGACTT-3′) was
482 used to determine the identity of the bacterial isolates.
483 ***Screening for pathogenic effects***
484 *M. brevicollis* was grown for 30 h, and feeding bacteria were reduced through
485 one round of centrifugation and resuspension in artificial seawater (ASW). Cells were
486 counted on a hemocytometer and diluted to $5x10^6$ cells/mL in High Nutrient Medium,
487 and plated into 24-well plates.
488 For each bacterium, a single colony was inoculated into LB and grown shaking
489 overnight at either 30º C (environmental isolates) or 37º C (mouse isolates). Bacterial
490 cells were pelleted by centrifugation for 5 minutes at 4000 x *g,* and resuspended in
491 artificial seawater (ASW) to an OD~1.
492 Each bacterial species was added to *M. brevicollis* culture at two concentrations
493 (10mL/mL and 50 mL/mL) in duplicate. *M. brevicollis* was then monitored at regular
494 intervals for changes in behavior and growth.
495 ***Growth curves in the presence of bacteria***
496 All bacteria were grown shaking at 30º C in Sea Water Complete media or LB (to
497 optical density of 0.8). For each bacterial strain, CFU plating was used to estimate the
498 number of bacterial cells/ mL under these growth conditions. To prepare bacterial
499 conditioned media, bacterial cells were pelleted by centrifugation for 10 minutes at 4000
500 x *g,* and supernatant was passed through a 0.22mm sterilizing filter.

501 *M. brevicollis* was grown for 30 h, and bacteria were washed away through two
502 consecutive rounds of centrifugation and resuspension in artificial seawater (ASW).
503 Cells were counted on a hemocytometer and diluted to $1.0x10^6$ cells/mL (growth curves
504 with live bacteria) or $1.5x10^5$ cells/mL (growth curves with conditioned medium) in High
505 Nutrient Medium. To test the effects of live bacteria, $1.5x10^6$ bacterial cells were added
506 per 1 mL of *M. brevicollis* culture. To test the effects of bacterial conditioned media, 50
507 ml of bacterial conditioned media was added per 1 mL of *M. brevicollis* culture. For each
508 growth curve biological replicate, cells were plated into 24-well plates, and two wells
509 were counted per time point as technical replicates. At least three biological replicates
510 are represented in each graph.

511 ***Bacterial internalization***

512 Fluorescent *E. coli* and *P. aeruginosa* were grown shaking at 30º C in LB to an
513 optical density of $OD_{600}$=0.8. Fluorescent *C. jejuni* was grown from freezer stocks in
514 microaerobic conditions on Mueller-Hinton agar. For each bacterial strain, CFU plating
515 was used to estimate the number of bacterial cells/ mL under these growth conditions.
516 *M. brevicollis* was grown for 30 h, and feeding bacteria were washed away with
517 one round of centrifugation and resuspension in artificial seawater (ASW). Cells were
518 counted and diluted to $1.5x10^5$ cells/mL in ASW. $1.5x10^7$ bacterial cells were added to 2
519 mL *M. brevicollis* culture (MOI=50), and co-incubated at room temperature for 1 hr with
520 gentle mixing at regular intervals to avoid settling. To quantify bead internalization, *M.*
521 *brevicollis* was co-incubated with bacteria for 1 hour (as described above), at which
522 point ~$1x10^{10}$ beads (0.2mm diameter, resuspended in 1% BSA to prevent clumping)
523 were added to the conical for an additional 30 minutes.
524 Prior to imaging, 200mL aliquots were transferred to 8-well glass bottom
525 chambers (Ibidi Cat. No 80827). Live imaging was performed on a Zeiss Axio Observer
526 widefield microscope using a 63x objective. Images were processed and analyzed using
527 Fiji[63].

528 ***P. aeruginosa deletion mutants***

529 *P. aeruginosa* deletion strains were acquired from the Seattle PAO1 transposon
530 mutant library (NIH P30 DK089507). Strains RP436 and RP576 (PMID 15731071) were
531 acquired from Russell Vance, The effects of both live bacteria and bacterial conditioned
532 medium were tested for all acquired strains at a range of PFU/mL (live bacteria) or
533 percent volume (conditioned medium).
534

535 <u>Immune agonist dose-response curves</u>

536 *M. brevicollis* was grown to late-log phase, and feeding bacteria were reduced
537 through one round of centrifugation and resuspension in artificial seawater (ASW). Cells
538 were counted on a hemocytometer and diluted to $1.0x10^6$ cells/mL (growth curves with
539 live bacteria) in High Nutrient Medium, and aliquoted into 96-well (100µL/well) or 24-well
540 (1mL/well) plates. Immune agonists were added at indicated concentrations in technical
541 duplicate, and cells were counted again after 24 hours. % survival is a calculation of:

542 [mean experimental (cells/mL) / mean control (cells/mL)]. Each dose-response curve is
543 representative of at least three biological replicates.
544
545 RNA-seq
546 ***Growth of choanoflagellate cultures***
547 After thawing new cultures, growth curves were conducted to determine the
548 seeding density and time required to harvest cells at late-log phase growth. To grow
549 large numbers of cells for RNA-seq, cells were seeded one to two days prior to the
550 experiment in either 3-layer flasks (Falcon; Corning, Oneonta, NY, USA; Cat. No. 14-
551 826-95) or 75 $cm^2$ flasks (Falcon; Corning, Oneonta, NY, USA; Cat. No. 13-680-65),
552 and grown at room temperature. Bacteria were washed away from choanoflagellate
553 cells through two rounds of centrifugation and resuspension in artificial seawater (ASW).
554 To count the cell density, cells were diluted 100-fold in 200 µl of ASW, and fixed with 1
555 µL of 16% paraformaldehyde. Cells were counted on a hemocytometer, and the
556 remaining cells were diluted to a final concentration of $4\times10^6$ choanoflagellate cells/mL.
557 The resuspended cells were divided into 2.5 mL aliquots and plated in 6-well plates
558 prior to treatment. After treatment, cells were transferred to a 15 mL conical and
559 pelleted by centrifugation at 2400 x *g* for 5 min, flash frozen with liquid nitrogen, and
560 stored at -80°C.
561 ***RNA isolation***
562 Total RNA was isolated from cell pellets with the RNAqueous kit (Ambion,
563 Thermo Fisher Scientific). Double the amount of lysis buffer was used to increase RNA
564 yield and decrease degradation, and RNA was eluted in minimal volumes in each of the
565 two elution steps (40 µL and 15 µL). RNA was precipitated in LiCl to remove
566 contaminating genomic DNA. Total RNA concentration and quality was evaluated using
567 the Agilent Bioanalyzer 2100 system and RNA Nano Chip kit (Cat No. 5067-1511).
568 ***Library preparation, sequencing, and analysis***
569 Libraries were prepared and sequenced by the UTSW Genomics Sequencing
570 Core. RNA libraries were generated with the Illumina TruSeq® Stranded mRNA Library
571 prep kit (Cat No. 20020594), using a starting total RNA input of 2-3 µg. To remove
572 contaminating bacterial RNA, samples were first poly-A selected using oligo-dT
573 attached magnetic beads. Following purification, the mRNA was fragmented at 94ºC for
574 4 minutes, and cleaved RNA fragments were synthesized into cDNA. After an end
575 repair step, UMI adapters (synthesized by IDT) were ligated to the cDNA, and the
576 products were twice purified using AMPure XP beads before amplification.
577 Library quantity was measured using the Quant-iT™ PicoGreen dsDNA Assay kit by
578 Invitrogen (Cat No. P7589) and a PerkinElmer Victor X3, 2030 Multilabel Reader.
579 Library quality was verified on an Agilent 2100 Bioanalyzer instrument using Agilent
580 High sensitivity DNA kit (Cat No. 5067-4626) or DNA 1000 kit (Cat No. 5067-
581 1504). Libraries were pooled, and sequenced in different batches on either the Illumina

582 NextSeq 550 system with SE-75 workflow, or the Illumina NovaSeq 6000 system with
583 S4 flowcell and XP PE-100 workflow, generating 25-40 million reads per sample. Reads
584 were checked for quality using fastqc (v0.11.2) and fastq_screen (v0.4.4), and trimmed
585 using fastq-mcf (ea-utils, v1.1.2-806). Trimmed fastq files were mapped to the *Monosiga*
586 *brevicollis* reference genome (NCBI:txid81824) using TopHat[64] (v2.0.12). Duplicates
587 were marked using picard-tools (v2.10.10). Read counts were generated using
588 featureCounts[65], and differential expression analysis was performed using edgeR[66].
589 Statistical cutoffs of FDR≤$10^{-4}$ were used to identify significant differentially expressed
590 genes. GO enrichment analysis of differentially expressed genes was performed using
591 DAVID (https://david.ncifcrf.gov/).
592
593 RT-qPCR
594 RNA was isolated as described above, and cDNA was synthesized from total
595 RNA with the High Capacity cDNA Reverse Transcription kit (Applied Biosystems;
596 Thermo Fisher. Real-time PCR was performed with iTaq Universal SYBR Green
597 Supermix (Biorad; Cat No. 1725121) or SYBR Green PCR master mix (Applied
598 Biosystems; Cat No. 4309155) in either an 7500 Fast Real-Time PCR System (Applied
599 Biosystems), or a QuantStudio 3 Real-Time PCR System (Applied Biosystems). Ct
600 values were converted into relative gene expression using the ΔΔCt method (Livak and
601 Schmittgen, 2001) and the internal control gene RPL15 (MONBRDRAFT_38309).
602
603 Immunoblotting
604 *M. brevicollis* was harvested by centrifugation at 5,000 x *g* for 5 min at 4°C, and
605 resuspended in 100 µL lysis buffer (50mM Tris, pH 7.4, 150 mM NaCl, 1 mM EDTA, 1
606 mM ethyleneglycoltetraacetic acid [EGTA], 0.5% sodium deoxycholate, 1% NP-40)
607 containing protease inhibitor cocktail (Roche) for 10 min at 4°C. The crude lysate was
608 clarified by centrifugation at 10,000 x *g* for 10 min at 4°C, and denatured in Laemmli
609 buffer before SDS-PAGE. Proteins were transferred to an Immobilon-P PVDF
610 membrane (Millipore), and blocked for two hours in PBST (1x PBS containing 5% nonfat
611 dry milk and 0.05% Tween-20). Membranes were incubated with primary antibodies
612 diluted in PBST overnight at 4°C and washed extensively in PBST. Membranes were
613 incubated with secondary antibodies for 1 hour at room temperature, washed
614 extensively in PBST, and developed using Immobilon Western Chemiluminescent HRP
615 Substrate (Millipore Sigma). Source data files for all western blots are provided as
616 Source Data File 1.
617 ***STING antibody production***
618 The anti-mbreSTING antibody was generated by Pacific Immunology. Rabbits
619 were immunized with a KLH-conjugated peptide corresponding to residues 320-338 of
620 *M. brevicollis* protein EDQ90889.1 (Cys-KNRSEVLKKMRAEDQYAMP), and serum was
621 affinity purified against the peptide to reduce cross-reactivity and validated using
622 immunoblotting.

623
624 Immunofluorescence Staining and Imaging
625 Depending on the cell density of the starting culture, between 0.2-1 mL of cells
626 were concentrated by centrifugation for 5 min at 2500 × *g*. The cells were resuspended
627 in 200 µl of artificial seawater and applied to poly-L-lysine–coated coverslips (Corning
628 Life Sciences; Cat. No.354085) placed at the bottom of each well of a 24-well cell
629 culture dish. After the cells were allowed to settle on the coverslip for 30 min, 150 µl of
630 the cell solution was gently removed from the side of the dish. All of the subsequent
631 washes and incubations during the staining procedure were performed by adding and
632 removing 200 µl of the indicated buffer.
633 Cells were fixed in two stages. First, 200 µl cold 6% acetone diluted in 4X PBS
634 was added for 5 min at room temperature. Next, 200 µl cold 8% paraformaldehyde
635 diluted in 4X PBS was added (yielding a final concentration of 4% paraformaldehyde),
636 and the fixative mixture was incubated for 15 min at room temperature. After fixation,
637 the coverslip was gently washed three times with 200 µl 4X PBS.
638 Cells were permeabilized by incubating in permeabilization buffer (4X PBS; 3%
639 [wt/vol] bovine serum albumin (BSA)-fraction V; 0.2% [vol/vol] Triton X-100) for 30 min.
640 After removing permeabilization buffer, the coverslip was incubated in primary antibody
641 for 1 hour at room temperature, and then washed three times in 4X PBS. The coverslip
642 was then incubated with secondary antibody for 1 hour at room temperature, and then
643 washed twice in 4X PBS. The coverslip was next incubated in 4 U/ml Phalloidin
644 (Thermo Fisher Scientific) for 30 min at room temperature, washed once in 4X PBS.
645 Lastly, the coverslip was incubated in 10 µg/ml Hoechst 33342 (Thermo Fisher
646 Scientific) for 5 min at room temperature, and then washed once with 4X PBS.
647 To prepare a slide for mounting, 10 µl of Pro-Long Gold (Thermo Fisher
648 Scientific) was added to a slide. The coverslip was gently removed from the well with
649 forceps, excess buffer was blotted from the side with a piece of filter paper, and the
650 coverslip was gently placed on the drop of Pro-Long diamond. The mounting media
651 cured overnight before visualization.
652 Images were acquired on either: (1) a Zeiss LSM 880 Airyscan confocal microscope
653 with a 63x objective by frame scanning in the superresolution mode (images processed
654 using the automated Airyscan algorithm (Zeiss)), or (2) a Nikon CSU-W1 SoRa spinning
655 disk confocal microscope with a 60x objective in SR mode (images processed using
656 Imaris).
657
658 Live-Cell Imaging
659 Cells transfected with fluorescent reporter plasmid were prepared for microscopy
660 by transferring 200 µl of cells to a glass-bottom dish or glass-bottom 8-well chamber
661 (Ibidi). Confocal microscopy was performed on a Zeiss Axio Observer LSM 880 with an
662 Fast Airyscan detector and a 63x/NA1.40 Plan-Apochromatic oil immersion objective

663 (Carl Zeiss AG, Oberkochen, Germany). Confocal stacks were acquired by frame
664 scanning in superresolution mode, and images were processed using the automated
665 Airyscan algorithm (Zeiss).
666
667 Transfection of *M. brevicollis*
668 ***Cell Culture.*** One day prior to transfection, 60 ml of High Nutrient Medium was
669 inoculated with *M. brevicollis* to a final concentration of 10000 cells/ml. The culture was
670 split in two, and grown in two 75 $cm^2$ flasks at room temperature, approximately 22°C
671 (Falcon; Corning, Oneonta, NY, USA; Cat. No. 13-680-65).
672 ***Cell Washing.*** After 24 hours of growth, bacteria were washed away from *M.*
673 *brevicollis* cells through three consecutive rounds of centrifugation and resuspension in
674 artificial seawater (ASW). The culture flasks were combined and vigorously shaken for
675 30 s, and then transferred to 50-ml conical tubes and spun for 5 min at 2000 × *g* and
676 22°C. The supernatant was removed with a serological pipette, and residual media were
677 removed with a fine-tip transfer pipette. The cell pellets were resuspended in a single
678 conical tube in a total volume of 50 ml of ASW, vigorously shaken for 30 s, and then
679 centrifuged for 5 min at 2050 × *g*. The supernatant was removed as before. In a final
680 washing step, the cell pellet was resuspended in 50 mL ASW, shaken vigorously, and
681 centrifuged for 5 min at 2100 × *g*. After the supernatant was removed, the cells were
682 resuspended in a total volume of 400 µl of ASW. To count the cell density, cells were
683 diluted 100-fold in 200 µl of ASW, and fixed with 1 µl of 16% paraformaldehyde. Cells
684 were counted on a hemocytometer, and the remaining cells were diluted to a final
685 concentration of $5 \times 10^7$ choanoflagellate cells/ml. The resuspended cells were divided
686 into 100-µl aliquots with $5 \times 10^6$ cells per aliquot to immediately prime cells in the next
687 step.
688 ***Cell Priming.*** Each aliquot of *M. brevicollis* cells was incubated in priming buffer (40
689 mM HEPES-KOH, pH 7.5; 55 mM lithium citrate; 50 mM L-cysteine; 10% [wt/vol] PEG
690 8000; and 2 µM papain) to remove the extracellular material coating the cell. The 100-µl
691 aliquots, which contained $5 \times 10^6$ cells, were centrifuged for 5 min at 1700 × *g*. The
692 supernatant was removed, and cells were resuspended in 100 µl of priming buffer and
693 then incubated for 35 min at room temperature. Priming was quenched by adding 4 µl of
694 50-mg/ml bovine serum albumin-fraction V (Thermo Fisher Scientific, Waltham, MA;
695 Cat. No. BP1600-100) and then centrifuged for 5 min at 1250 ×*g* and 22°C with the
696 centrifuge brake set to a "soft" setting. The supernatant was removed with a fine-tip
697 micropipette, and the cells were resuspended in 25 µl of SG Buffer (Lonza).
698 ***Nucleofection.*** Each transfection reaction was prepared by adding 2 µl of "primed"
699 cells resuspended in SG buffer (Lonza) to a mixture of: 16 µl of SG buffer, 2 µl of 20
700 µg/µl pUC19, 1 µl of 250 mM ATP (pH 7.5), 1 µl of 100 mg/ml sodium heparin, and ≤7 µl
701 of reporter DNA (volume is dependent on the number of constructs transfected). Each
702 transfection reaction was transferred to one well in 16-well nucleofection strip (Lonza;

703 Cat. No. V4XC-2032). The nucleofection strip was placed in the X-unit (Lonza; Cat. No.
704 AAF-1002F) connected to a Nucleofector 4D core unit (Lonza; Cat. No. AAF-1002B),
705 and the EO100 pulse was applied to each well.
706 ***Recovery.*** 100 µl of cold recovery buffer (10 mM HEPES-KOH, pH 7.5; 0.9 M
707 sorbitol; 8% [wt/vol] PEG 8000) was added to the cells immediately after pulsation. After
708 5 minutes, the whole volume of the transfection reaction plus the recovery buffer was
709 transferred to 2 ml of Low Nutrient Medium in a 12-well plate. The cells were grown for
710 24–48 hours before being assayed for luminescence or fluorescence.
711 ***Puromycin Selection.*** To generate stably transfected *M. brevicollis* cell lines,
712 puromycin was added to cells 24 hours after transfection at a final concentration of 300
713 µg/mL. Cells were monitored over the course of 7-21 days, and fresh High Nutrient
714 Media + 300 µg/mL puromycin was added to the cells as needed.
715
716 Genome editing
717 For a more detailed description of gRNA and repair oligonucleotide design, refer to
718 Booth et al. 2018[50].
719 ***Design and preparation of gRNAs*** First, crRNAs were designed by using the
720 extended recognition motif 5'-HNNGRSGGH-3' (in which the PAM is underlined, N
721 stands for any base, R stands for purine, S stands for G or C, and H stands for any
722 base except G) to search for targets in cDNA sequences[67]. Next, we confirmed that the
723 RNA sequence did not span exon-exon junctions by aligning the sequence to genomic
724 DNA.
725 Functional gRNAs were prepared by annealing synthetic crRNA with a synthetic
726 tracrRNA[52]. To prepare a functional gRNA complex from synthetic RNAs, crRNA and
727 tracrRNA (Integrated DNA Technologies [IDT], Coralville, IA, USA) were resuspended
728 to a final concentration of 200 µM in duplex buffer (30 mM HEPES-KOH, pH 7.5; 100
729 mM potassium acetate; IDT, Cat. No. 11-0103-01). Equal volumes of crRNA and
730 tracrRNA stocks were mixed together, incubated at 95°C for 5 min in an aluminum
731 block, and then the entire aluminum block was placed at room temp to slowly cool the
732 RNA to 25°C. The RNA was stored at -20°C
733 ***Design and preparation of repair oligonucleotides*** Repair oligonucleotides for
734 generating knockouts were designed by copying the sequence 50 bases upstream and
735 downstream of the SpCas9 cleavage site. A knockout sequence
736 (5'TTTATTTAATTAAATAAA-3') was inserted at the cleavage site[52].
737 Dried oligonucleotides (IDT) were resuspended to a concentration of 250 µM in a
738 buffer of 10 mM HEPES-KOH, pH 7.5, incubated at 55°C for 1 hour, and mixed well by
739 pipetting up and down. The oligonucleotides were stored at -20°C.
740 ***Delivery of gene editing cargoes with nucleofection***
741 The method for delivering *Sp*Cas9 RNPs and DNA repair templates into *M.*
742 *brevicollis* is as follows:

743 ***Cell Culture.*** One day prior to transfection, 60 ml of High Nutrient Medium was
744 inoculated to a final concentration of *M. brevicollis* at 10000 cells/ml. The culture was
745 split in two, and grown in two 75 $cm^2$ flasks at room temperature, approximately 22°C
746 (Falcon; Corning, Oneonta, NY, USA; Cat. No. 13-680-65).
747 ***Assembly of Cas9/gRNA RNP.*** Before starting transfections, the *Sp*Cas9 RNP was
748 assembled. For one reaction, 2 µl of 20 µM *Sp*Cas9 (NEB, Cat. No. M0646M) was
749 placed in the bottom of a 0.25 ml PCR tube, and then 2 µl of 100 µM gRNA was slowly
750 pipetted up and down with *Sp*Cas9 to gently mix the solutions. The mixed solution was
751 incubated at room temperature for 1 hour, and then placed on ice.
752 ***Thaw DNA oligonucleotides.*** Before using oligonucleotides in nucleofections, the
753 oligonucleotides were incubated at 55°C for 1 hour.
754 ***Cell Washing.*** After 24 hours of growth, bacteria were washed away from *M.*
755 *brevicollis* cells through three consecutive rounds of centrifugation and resuspension in
756 artificial seawater (ASW). The culture flasks were combined and vigorously shaken for
757 30 s, and then transferred to 50-ml conical tubes and spun for 5 min at 2000 × *g* and
758 22°C. The supernatant was removed with a serological pipette, and residual media were
759 removed with a fine-tip transfer pipette. The cell pellets were resuspended in a single
760 conical tube in a total volume of 50 ml of ASW, vigorously shaken for 30 s, and then
761 centrifuged for 5 min at 2050 × *g*. The supernatant was removed as before. In a final
762 washing step, the cell pellet was resuspended in 50 mL ASW, shaken vigorously, and
763 centrifuged for 5 min at 2100 × *g*. After the supernatant was removed, the cells were
764 resuspended in a total volume of 400 µl of ASW. To count the cell density, cells were
765 diluted 100-fold in 200 µl of ASW, and fixed with 1 µl of 16% paraformaldehyde. Cells
766 were counted on a hemocytometer, and the remaining cells were diluted to a final
767 concentration of $5 \times 10^7$ choanoflagellate cells/ml. The resuspended cells were divided
768 into 100-µl aliquots with $5 \times 10^6$ cells per aliquot to immediately prime cells in the next
769 step.
770 ***Cell Priming.*** Each aliquot of *M. brevicollis* cells was incubated in priming buffer (40
771 mM HEPES-KOH, pH 7.5; 50 mM lithium citrate; 50 mM L-cysteine; 15% [wt/vol] PEG
772 8000; and 2 µM papain) to remove the extracellular material coating the cell. The 100-µl
773 aliquots, which contained $5 \times 10^6$ cells, were centrifuged for 5 min at 1700 × *g* and at
774 room temperature. The supernatant was removed, and cells were resuspended in 100
775 µl of priming buffer and then incubated for 35 min. Priming was quenched by adding 10
776 µl of 50-mg/ml bovine serum albumin-fraction V (Thermo Fisher Scientific, Waltham,
777 MA; Cat. No. BP1600-100). Cells were then centrifuged for 5 min at 1250 ×*g* and 22°C
778 with the centrifuge brake set to a "soft" setting. The supernatant was removed with a
779 fine-tip micropipette, and the cells were resuspended in 25 µl of SG Buffer (Lonza).
780 ***Nucleofection.*** Each nucleofection reaction was prepared by adding 16 µl of cold
781 SG Buffer to 4 µl of the *Sp*Cas9 RNP that was assembled as described above. For
782 reactions that used two different guide RNAs, each gRNA was assembled with *Sp*Cas9

separately and 4 µl of each RNP solution were combined at this step. 2 µl of the repair oligonucleotide template was added to the *Sp*Cas9 RNP diluted in SG buffer. Finally, 2 µl of primed cells were added to the solution with Cas9 RNP and the repair template. The nucleofection reaction was placed in one well of a 16-well nucleofection strip (Lonza; Cat. No. V4XC-2032). The nucleofection strip was placed in the X-unit (Lonza; Cat. No. AAF-1002F) connected to a Nucleofector 4D core unit (Lonza; Cat. No. AAF-1002B), and the EO100 pulse was applied to each well.

***Recovery.*** 100 µl of cold recovery buffer (10 mM HEPES-KOH, pH 7.5; 0.9 M sorbitol; 8% [wt/vol] PEG 8000) was added to the cells immediately after pulsation. After 5 minutes, the whole volume of the transfection reaction plus the recovery buffer was transferred to 1 ml of High Nutrient Medium in a 12-well plate.

***Cycloheximide Selection in M. brevicollis.*** One day after transfection, 10 µl of 10 µg/ml cycloheximide was added per 1 mL culture of transfected cells. The cells were incubated with cycloheximide for 5 days prior to clonal isolation and genotyping.

***Genotyping***. Cells were harvested for genotyping by spinning 0.5ml of cells at 4000*g* and 22°C for 5 min. The supernatant was removed and DNA was isolated either by Base-Tris extraction [in which the cell pellet was resuspended in 20uL base solution (25mM NaOH, 2mM EDTA), boiled at 100°C for 20 min, cooled at 4°C for 5 min, and neutralized with 20uL Tris solution (40mM Tris-HCl, pH 7.5)], or by DNAzol Direct [in which the cell pellet was resuspended in 50uL and incubated at room temperature for 30 min (Molecular Research Center, Inc. [MRC, Inc.], Cincinnati, OH; Cat. No. DN131)]. 3 µl of the DNA solution was added to a 25 µl PCR reaction (DreamTaq Green PCR Master Mix, Thermo Fisher Scientific Cat No K1082) and amplified with 34 rounds of thermal cycling.

## Data Availability

Source data files for all western blots are provided in Source Data File 1. Raw sequencing reads and normalized gene counts for all RNA-seq experiments have been deposited at the NCBI GEO under accession GSE174340.

815 **Figure Legends**
816
817 **Figure 1. *P. aeruginosa* has pathogenic effects on *M. brevicollis***
818 **(A)** Immunofluorescence illuminates the diagnostic cellular architecture of *M. brevicollis*,
819 including an apical flagellum (f) made of microtubules, surrounded by an actin-filled
820 microvilli feeding collar (co). Staining for tubulin (green) also highlights cortical
821 microtubules that run along the periphery of the cell body, and staining for F-actin
822 (magenta) highlights basal filopodia (fp). DNA staining (blue) highlights the nucleus (n).
823 **(B)** *M. brevicollis* exhibits truncated flagella after exposure to *P. aeruginosa. M.*
824 *brevicollis* were exposed to *E. coli* or *P. aeruginosa* for 24 hours, and then fixed and
825 immunostained. Arrows point to flagella. Green: anti-tubulin antibody (flagella and cell
826 body), magenta: phalloidin (collar), blue: Hoechst (bacterial and choanoflagellate
827 nuclei). Scale bars represent 10μm. Flagellar length was quantified using Fiji, and
828 statistical analysis (unpaired t-tests) was performed in GraphPad software. **(C)**
829 Exposure to *P. aeruginosa*, but not other Gammaproteobacteria, results in *M. brevicollis*
830 cell death. Bacteria were added to *M. brevicollis* culture at an MOI of 1.5 (at Hours=0),
831 and *M. brevicollis* cell density was quantified at indicated time points. Data represent
832 mean +/- SD for three biological replicates. Statistical analysis (multiple unpaired t-tests)
833 was performed in GraphPad software; *p*-values shown are from comparisons between
834 *Flavobacterium* and *P. aeruginosa.* (**D-F)** *M. brevicollis* does not ingest *P. aeruginosa*
835 bacteria. **(D,E)** *M. brevicollis* were fed either fluorescent *E. coli* (D) or *P. aeruginosa* (E)
836 for one hour, and then visualized by DIC (D,E, left) and green fluorescence (D, E, right).
837 Fluorescent food vacuoles were observed in choanoflagellates fed *E. coli,* but not *P.*
838 *aeruginosa.* **(F)** *M. brevicollis* was exposed to GFP-expressing *E. coli*, *V.*
839 *parahaemolyticus*, *C. jejuni*, or *P. aeruginosa* (MOI=50) for one hour, and then imaged
840 by DIC and green fluorescence to quantify number of cells with internalized bacteria.
841 Choanoflagellate cells with ≥1 GFP+ food vacuole were scored as GFP+, and cells
842 without any GFP+ food vacuoles were scored as GFP–. Data represent cells quantified
843 over three biological replicates. **(G,H)** *P. aeruginosa* does not broadly inhibit *M.*
844 *brevicollis* phagocytosis. **(G)** Internalization of 0.2μm fluorescent beads was used to
845 quantify phagocytic activity after exposure to *E. coli* or *P. aeruginosa* bacteria. Although
846 cells did not phagocytose *P. aeruginosa,* cells exposed to *E. coli* and *P. aeruginosa* had
847 similar phagocytic uptake of beads. Data represent n=600 cells from three biological
848 replicates. Statistical analyses (multiple unpaired t-tests) were performed in GraphPad
849 software. **(H)** Exposure to *P. aeruginosa* does not inhibit phagocytic uptake of *E. coli.*
850 Internalization of fluorescent *E. coli* or *P. aeruginosa* bacteria was quantified after
851 exposure to unlabeled *P. aeruginosa* (PAO1 strain). Data represent n=200 cells from
852 two biological replicates. Statistical analysis (unpaired t-test) was performed in
853 GraphPad software. **(I)** Secreted *P. aeruginosa* molecules are sufficient to induce *M.*
854 *brevicollis* cell death. 5% (vol/vol) bacterial conditioned medium was added to *M.*

855 *brevicollis* culture (at Hours=0), and *M. brevicollis* cell density was quantified at
856 indicated time points. Data represent mean +/- SD for three biological replicates.
857 Statistical analysis (multiple unpaired t-tests) was performed in GraphPad software, and
858 *p*-values shown are from comparisons between *Flavobacterium* and *P. aeruginosa.* **(J)**
859 Sustained exposure to secreted *P. aeruginosa* molecules is required to induce *M.*
860 *brevicollis* cell death. *P. aeruginosa* or *Flavobacterium* conditioned medium (5% vol/vol)
861 was added to stationary-phase *M. brevicollis* cultures. After indicated times, cultures
862 were washed and resuspended in fresh media. *M. brevicollis* cell density was quantified
863 after 24 hours. The % survival is a measure of the cell density of *P. aeruginosa*-treated
864 cells relative to *Flavobacterium*-treated controls. Data represent mean +/- SD for three
865 biological replicates.
866
867
868
869 **Figure 1 – figure supplement 1. Presence of animal innate immune genes in**
870 **choanoflagellates (A)** The transcriptomes of 21 choanoflagellate species[3] were
871 searched for genes that play key roles in animal innate immune responses. Evidence
872 for gene presence was based on sequence homology in a BLAST-based approach and
873 conserved domain architectures, as described in Richter et al., 2018.
874
875 **Video 1, Supplementary file 1. *P. aeruginosa* influences *M. brevicollis* motility.**
876 Movies depicting *M. brevicollis* cultures after exposure to *E. coli* or *P. aeruginosa*
877 bacteria for 16 hours. In the absence of pathogenic bacteria, like *E. coli*, M. *brevicollis* is
878 a highly motile flagellate and swims up in the water column. However, co-culturing *M.*
879 *brevicollis* with *P. aeruginosa* results in reduced motility and cell settling.
880
881 **Figure 2. STING is upregulated in *M. brevicollis* after exposure to *P. aeruginosa***
882 **(A,B)** *STING* transcript levels increase in response to *P. aeruginosa.* **(A)** Volcano plot
883 displaying genes differentially expressed between *M. brevicollis* exposed to *P.*
884 *aeruginosa* PAO1 and *Flavobacterium* (control) conditioned medium for three hours.
885 Differentially expressed genes are depicted by blue (674 upregulated genes) and yellow
886 (232 downregulated genes) dots (fold change≥2; FDR≤$1e^{-4}$). Select genes that are
887 upregulated or may function in innate immunity are labeled. RNA-seq libraries were
888 prepared from four biological replicates. **(B)** After a three-hour treatment, *STING* mRNA
889 levels (determined by RNA-seq) increase 1.42 fold in cells exposed to *Flavobacterium*
890 conditioned medium and 5.54 fold in cells exposed to *P. aeruginosa* conditioned
891 medium, compared to untreated controls. **(C)** STING protein levels increase after
892 exposure to *P. aeruginosa*. STING levels were examined by immunoblotting at indicated
893 timepoints after exposure to *Flavobacterium* or *P. aeruginosa* conditioned medium (5%
894 vol/vol). Tubulin is shown as loading control, and intensity of STING protein bands were

895 quantified relative to tubulin. Statistical analysis (one-way ANOVA, Dunnett's multiple
896 comparison) was performed in GraphPad software, and *p*-values shown are calculated
897 using 0 hour timepoint as the control group.
898
899
900
901 **Figure 2 – figure supplement 2. *M. brevicollis* response to *P. aeruginosa,* and**
902 **STING antibody validation and protein alignment. (A)** Gene ontology enrichment
903 analysis of genes identified as differentially expressed (fold change≥2; FDR≤$1e^{-4}$) after
904 exposure to *P. aeruginosa*. Due to lack of annotation, >40% of the differentially
905 expressed genes were not included in the enrichment analysis. **(B)** qRT-PCR validation
906 of *STING* mRNA after exposure to *Flavobacterium* or *P. aeruginosa* conditioned media
907 for three hours, compared to vehicle control. Error bars represent SD. Statistical
908 analysis (t-test) was performed in GraphPad software **(C)** To validate the *M. brevicollis*
909 STING antibody, cell lysates from *M. brevicollis* were immunoblotted alongside cell
910 lysates from *S. rosetta,* a closely-related choanoflagellate species that does not have a
911 STING homolog. A band at 36kD, the predicted size of *M. brevicollis* STING, is
912 detectable in *M. brevicollis* lysate but not *S. rosetta* lysate. Arrow indicates STING band.
913 Non-specific bands are likely due to co-cultured feeding bacteria. Tubulin is shown as
914 loading control. **(D)** Protein sequence alignment (generated by Clustal Omega multiple
915 sequence alignment) of *M. brevicollis* and animal STING proteins, colored by similarity.
916 *M. brevicollis* STING and human STING are 19.1% identical and 36.6% similar at the
917 amino acid level.
918
919
920
921 **Figure 3. 2'3' cGAMP, but not bacterially-produced cyclic dinucleotides, induces**
922 **elevated levels of STING**
923 **(A)** Schematic of choanoflagellate (*M. brevicollis*), sea anemone (*N. vectensis*), insect
924 (*D. melanogaster*) and mammalian (*M. musculus* and *H. sapiens*) STING proteins.
925 Transmembrane (TM) domains are depicted in gray, STING cyclic dinucleotide binding
926 domain (CDN) in purple, and C-terminal tail domain (CTT) in blue. **(B)** Partial protein
927 sequence alignment (generated by Clustal Omega multiple sequence alignment) of *M.*
928 *brevicollis* and animal STING proteins, colored by similarity. *M. brevicollis* STING and
929 human STING are 19.1% identical and 36.6% similar at the amino acid level. Key cyclic
930 dinucleotide-interacting residues from human STING structure are indicated by circles.
931 **(C)** Dose-response curves of *M. brevicollis* exposed to cyclic dinucleotides for 24 hours
932 reveal that treatment with 2'3'cGAMP, but not 3'3' cGAMP, c-di-AMP, or c-di-GMP,
933 leads to *M. brevicollis* cell death in a dose-dependent manner. Data represent mean +/-
934 SD for at least three biological replicates. **(D)** STING protein levels increase after

935 exposure to 2'3'cGAMP, but not bacterially-produced cyclic dinucleotides. *M. brevicollis*
936 STING levels were examined by immunoblotting 5 hours after exposure to 2'3'cGAMP
937 (100 μM), 3'3'cGAMP (200 μM), c-di-GMP (200 μM), or c-di-AMP (200 μM). Tubulin is
938 shown as loading control, and intensity of STING protein bands were quantified relative
939 to tubulin. Shown is a representative blot from three biological replicates. Statistical
940 analysis (one-way ANOVA, Dunnett's multiple comparison) was performed in GraphPad
941 software. **(E)** STING protein levels increase and remain elevated after exposure to 100
942 μM 2'3'cGAMP. Tubulin is shown as loading control, and data are representative of
943 three biological replicates. Statistical analysis (one-way ANOVA, Dunnett's multiple
944 comparison) was performed in GraphPad software, and *p*-values shown are calculated
945 using 0 hour timepoint as control group.
946
947
948
949 **Figure 3 – figure supplement 1. *M. brevicollis* has distinct responses to 2'3'**
950 **cGAMP and 3'3' cGAMP**
951 **(A,B)** Volcano plots displaying RNA-seq differential expression analysis of *M. brevicollis*
952 treated with (A) 100 μM 2'3'cGAMP or (B) 200 μM 3'3'cGAMP for 3 hours, relative to an
953 untreated control. Genes with a fold change ≥2 and false discovery rate ≤$10e^{-4}$ are
954 depicted by black dots. STING is highlighted in red. RNA-seq libraries were prepared
955 from three (2'3' cGAMP) or two (3'3' cGAMP) biological replicates. **(C)** *M. brevicollis*
956 *STING* mRNA levels increase in response to 2'3'cGAMP. (Left) RNA-seq fold change of
957 *STING* mRNA after exposure to 100 μM 2'3'cGAMP or 200 μM 3'3'cGAMP for three
958 hours, compared to vehicle control. (Right) qRT-PCR fold change of *STING* mRNA after
959 exposure to 100 μM 2'3'cGAMP or 200 μM 3'3'cGAMP for three hours, compared to
960 vehicle control. **(D)** Venn diagram comparing the overlap of genes identified as
961 differentially expressed after treatment with 2'3'cGAMP, 3'3'cGAMP, and *P. aeruginosa*
962 (DEG cutoff: fold change ≥ 3, false discovery rate ≤ $10e^{-4}$). (**E,F)** Representative
963 immunostained *M. brevicollis* demonstrating 2'3'cGAMP stimulates the formation of
964 STING puncta at perinuclear regions. *M. brevicollis* was left untreated (E), or exposed to
965 100 μM 2'3'cGAMP (F) for 5 hours. Cells were fixed and STING levels and localization
966 were probed using an anti-STING antibody. **(E',F')** Exposure to 2'3'cGAMP results in
967 increased numbers of STING puncta compared to untreated controls. **(E'',F'')** Z-slice
968 images of the plane containing the nucleus 'n' show that STING puncta localize to
969 perinuclear regions. Green: anti-tubulin antibody (flagella and cell body), magenta: anti-
970 STING antibody, blue: Hoechst. Scale bar represents 2 μm.
971
972
973

974 **Figure 4. Transfection reveals STING localization to perinuclear and endoplasmic**
975 **reticulum regions**
976 **(A)** STING-mTFP localizes to tubule-like structures around the nucleus in cells stably
977 expressing STING-mTFP. Green: anti-tubulin antibody (flagella and cell body),
978 magenta: anti-STING antibody, blue: Hoechst. Scale bar represents 2 µm. **(B,C)**
979 Fluorescent markers and live cell imaging reveal that STING is localized to the
980 endoplasmic reticulum (ER). Cells were co-transfected with STING-mTFP and an
981 mCherry fusion protein that localizes either to the endoplasmic reticulum (B; mCherry-
982 HDEL) or mitochondria (C; Cox4-mCherry )[4]. Cells were recovered in the presence of
983 *Flavobacterium* feeding bacteria for 28 hours after co-transfection, and then live cells
984 were visualized with super-resolution microscopy. Each panel shows Z-slice images of
985 a single representative cell. In confocal Z-slice images, cells are oriented with the apical
986 flagella pointing up, and the nucleus is marked by 'n' when clearly included in the plane
987 of focus. STING colocalized with the ER marker (B''), but not the mitochondrial marker
988 (C''). Scale bar represents 2 µm.
989
990
991
992 **Figure 5. STING mediates responses to 2'3'cGAMP and *P. aeruginosa***
993 **(A)** The genotypes of wild type and genome-edited *STING*$^{-}$ strains at the *STING* locus.
994 **(B)** STING protein is not detectable by immunoblot in *STING*$^{-}$ cells. Shown is a
995 representative blot from three biological replicates. **(C,D)** STING is necessary for
996 2'3'cGAMP-induced cell death. **(C)** Wild type and *STING*$^{-}$ strains were treated with
997 increasing concentrations of 2'3'cGAMP, and survival was quantified after 24 hours. In
998 contrast to wild type cells, 2'3'cGAMP does not induce cell death in *STING*$^{-}$ cells. Data
999 represent mean +/- SD for four biological replicates. **(D)** Wild type and *STING*$^{-}$ cells
1000 were transfected with STING-mTFP, and treated with puromycin to generate stable
1001 clonal strains. Stable expression of STING-mTFP in *STING*$^{-}$ cells partially rescued the
1002 phenotype of 2'3'cGAMP-induced cell death. Data represent mean +/- SD for three
1003 biological replicates. Statistical analysis (multiple unpaired t-tests) was performed in
1004 GraphPad software. **(E)** Wild type and *STING*$^{-}$ strains have distinct transcriptional
1005 responses to 2'3' cGAMP. Differential expression analysis was performed on wild type
1006 and *STING*$^{-}$ cells treated with 100µM 2'3'cGAMP or a vehicle control for three hours. A
1007 heatmap comparing the $\log_2$ fold change of genes identified as differentially expressed
1008 (FC ≥2; FDR≤$10^{-4}$) in wild type cells after 2'3' cGAMP treatment, to their $\log_2$ fold
1009 change in *STING*$^{-}$ cells after 2'3' cGAMP treatment. RNA-seq libraries were prepared
1010 from two biological replicates. **(F)** Presence of STING in the transcriptomes of diverse
1011 choanoflagellate species. Data from Richter et al. 2018[3]. **(G)** Effects of 2'3'cGAMP on
1012 different choanoflagellate species. Choanoflagellates were grown to late-log phase, and
1013 treated with increasing concentrations of 2'3'cGAMP. Survival was quantified after 24

1014 hours. 2'3'cGAMP only affected the survival of *M. brevicollis* and *S. macrocollata*, the
1015 two sequenced choanoflagellate species with a STING homolog. Data represent mean
1016 +/- SD for three biological replicates. **(H)** Wild type and *STING*$^{-}$ cells have similar
1017 survival responses to LPS, suggesting that STING is not required for mediating a
1018 response to LPS. Wild type and *STING*$^{-}$ strains were treated with increasing
1019 concentrations of *E. coli* LPS, and survival was quantified after 24 hours. Data represent
1020 mean +/- SD for four biological replicates. Statistical analysis (multiple unpaired t-tests)
1021 was performed in GraphPad software. **(I,J)** STING renders *M. brevicollis* more
1022 susceptible to *P. aeruginosa*-induced growth inhibition. **(I)** Wild type and *STING*$^{-}$ cells
1023 were exposed to control *Flavobacterium* or *P. aeruginosa* conditioned medium (5%
1024 vol/vol), and cell densities were quantified at indicated time points. Data represent mean
1025 +/- SD for three biological replicates. **(J)** Percent survival calculated from growth curves
1026 in (I). Statistical analysis (multiple unpaired t-tests) was performed in GraphPad
1027 software.
1028
1029
1030
1031 **Figure 5- figure supplement 1. Characterizing *STING*$^{-}$ *M. brevicollis***
1032 **(A)** Sanger sequences of the consensus genotype at the site of gene editing in wild type
1033 and *STING*$^{-}$ cells. *STING*$^{-}$ cells have a 7 base-pair deletion that leads to premature stop
1034 codons. **(B)** Growth curves of wild type and *STING*$^{-}$ cells indicate that both strains have
1035 similar growth dynamics. Statistical analysis (multiple unpaired t-tests) was performed in
1036 GraphPad software. **(C)** Volcano plot displaying RNA-seq differential expression
1037 analysis of *STING*$^{-}$ cells treated with 100 μM 2'3'cGAMP for 3 hours, relative to an
1038 untreated control. Genes with a fold change ≥2 and false discovery rate ≤$10e^{-4}$ are
1039 depicted by black dots. RNA-seq libraries were prepared from two biological replicates.
1040 **(D)** Venn diagram comparing the overlap of genes identified as differentially expressed
1041 (FC ≥3; FDR≤$10^{-4}$) after treatment with 2'3'cGAMP in wild type and *STING*$^{-}$ cells. **(E)**
1042 Protein sequence alignment (generated by Clustal Omega multiple sequence
1043 alignment) of STING proteins from choanoflagellates *S. macrocollata* and *M. brevicollis*
1044 and animals, colored by similarity.
1045
1046
1047
1048 **Figure 6. STING mediates 2'3'cGAMP-induced autophagic pathway**
1049 **(A)** 2'3'cGAMP-induced Atg8 lipidation requires STING. WT and *STING*$^{-}$ cells stably
1050 expressing mCherry-Atg8 were treated with a vehicle control or 100 μM 2'3'cGAMP for
1051 3 hours, followed by immunoblotting. The band intensity of Atg8-I (unmodified Atg8) and
1052 Atg8-II (lipidated Atg8) were quantified for each sample. Relative levels of Atg8
1053 lipidation were assessed by dividing the band intensities of Atg8-II/Atg8-I. Tubulin is

1054 shown as loading control. Immunoblot is representative of three biological replicates.
1055 **(B)** 2'3'cGAMP induces Atg8 lipidation in chloroquine-treated wild type cells. WT cells
1056 stably expressing mCherry-Atg8 were first incubated with 40 mM chloroquine for 6
1057 hours, and then treated with a vehicle control or 100 μM 2'3'cGAMP for 3 hours in the
1058 presence of chloroquine, followed by immunoblotting. For each sample, relative levels
1059 of Atg8 lipidation were assessed by dividing the band intensities of Atg8-II/Atg8-I.
1060 Tubulin is shown as loading control. Immunoblot is representative of three biological
1061 replicates. For a representative immunoblot and quantification of Atg8-II/Atg8-I levels in
1062 chloroquine-treated *STING*$^{-}$ cells, refer to Figure 6 - figure supplement 1B. **(C-G)**
1063 STING is required for 2'3'cGAMP-induced autophagosome formation. **(C-F)** WT and
1064 *STING*$^{-}$ cells stably expressing mCherry-Atg8 were treated with a vehicle control or 100
1065 μM 2'3'cGAMP for 3 hours, and then fixed and immunostained. **(C,D)** Representative
1066 confocal images of wild type cells show that Atg8 puncta accumulate after 2'3'cGAMP
1067 treatment. Magenta: mCherry-Atg8; Green: anti-tubulin antibody (flagella and cell body).
1068 **(E,F)** Representative confocal images of *STING*$^{-}$ cells show that Atg8 remains evenly
1069 distributed in the cytoplasm after 2'3'cGAMP treatment. **(G)** The number of Atg8
1070 puncta/cell was quantified for WT and *STING*$^{-}$ cells treated with a vehicle control or
1071 2'3'cGAMP for three hours. Data represent cells quantified from two biological replicates
1072 (n=150 cells per treatment group). Statistical analyses (unpaired two-tailed t-tests) were
1073 performed in GraphPad software. **(H)** Treatment with lysosomotropic agents that inhibit
1074 autophagy rescue 2'3' cGAMP-induced cell death in wild type cells. WT and *STING*$^{-}$
1075 cells were pre-treated with 40 mM chloroquine, 10mM $NH_4Cl$, or a vehicle control for 6
1076 hours. Cells were then exposed to either 100 μM 2'3'cGAMP or a vehicle control for 18
1077 hours before quantifying survival. Data represent mean +/- SD for three biological
1078 replicates. Statistical analyses (multiple unpaired t-tests) were performed in GraphPad
1079 software.
1080
1081
1082 **Figure 6 – figure supplement 1. STING mediates 2'3'cGAMP-induced autophagic**
1083 **signaling**
1084 **(A)** Overexpression of mCherry-Atg8 does not alter the susceptibility of wild type and
1085 *STING*$^{-}$ strains to 2'3'cGAMP. Wild type and *STING*$^{-}$ strains stably expressing mCherry-
1086 Atg8 were treated with increasing concentrations of 2'3'cGAMP, and survival was
1087 quantified after 24 hours. Data represent mean +/- SD for two biological replicates. **(B)**
1088 2'3'cGAMP does not induce increased Atg8 lipidation in chloroquine-treated *STING*$^{-}$
1089 cells. *STING*$^{-}$ cells stably expressing mCherry-Atg8 were incubated with 40 mM
1090 chloroquine for 6 hours, and then treated with a vehicle control or 100 μM 2'3'cGAMP
1091 for 3 hours in the presence of chloroquine, followed by immunoblotting. For each
1092 sample, relative levels of Atg8 lipidation were assessed by dividing the band intensities
1093 of Atg8-II/Atg8-I. Tubulin is shown as loading control. Immunoblot is representative of

1094 three biological replicates. Statistical analyses (unpaired two-tailed t-tests) were
1095 performed in GraphPad software.
1096
1097 **Source data file 1.** Uncropped western blots for: Figure 2- figure supplement 1C,
1098 Figure 2C, Figure 3D, Figure 3E, Figure 5B, Figure 6A, Figure 6B, Figure 6-
1099 supplement1B

## References


1. Shabalina, S. A. & Koonin, E. V. Origins and evolution of eukaryotic RNA interference. *Trends Ecol Evol* **23**, 578–587 (2008).

2. Richter, D. J. & Levin, T. C. The origin and evolution of cell-intrinsic antibacterial defenses in eukaryotes. *Curr Opin Genet Dev* **58–59**, 111–122 (2019).

3. Richter, D. J., Fozouni, P., Eisen, M. B. & King, N. Gene family innovation, conservation and loss on the animal stem lineage. *Elife* **7**, 946 (2018).

4. King, N. *et al.* The genome of the choanoflagellate Monosiga brevicollis and the origin of metazoans. *Nature* **451**, 783 788 (2008).

5. Brunet, T. & King, N. The Origin of Animal Multicellularity and Cell Differentiation. *Dev Cell* **43**, 124 140 (2017).

6. Richter, D. J. & King, N. The genomic and cellular foundations of animal origins. *Annu Rev Genet* **47**, 509 537 (2013).

7. Leadbeater, B. S. C. *The Choanoflagellates: Evolution, Ecology, and Biology*. (Cambridge University Press, 2015).

8. Dayel, M. J. & King, N. Prey capture and phagocytosis in the choanoflagellate Salpingoeca rosetta. *Plos One* **9**, e95577 (2014).

9. Wu, X. *et al.* Molecular evolutionary and structural analysis of the cytosolic DNA sensor cGAS and STING. *Nucleic Acids Res* **42**, 8243–8257 (2014).

10. Levin, T. C., Greaney, A. J., Wetzel, L. & King, N. The Rosetteless gene controls development in the choanoflagellate S. rosetta. *Elife* **3**, (2014).

11. Ablasser, A. & Chen, Z. J. cGAS in action: Expanding roles in immunity and inflammation. *Science* **363**, eaat8657 (2019).

12. Ahn, J. & Barber, G. N. STING signaling and host defense against microbial infection. *Exp Mol Medicine* **51**, 1–10 (2019).

13. Margolis, S. R., Wilson, S. C. & Vance, R. E. Evolutionary Origins of cGAS-STING Signaling. *Trends Immunol* **38**, 733–743 (2017).

14. Kranzusch, P. J. *et al.* Ancient Origin of cGAS-STING Reveals Mechanism of Universal 2′,3′ cGAMP Signaling. *Mol Cell* **59**, 891 903 (2015).

15. Ishikawa, H. & Barber, G. N. STING is an endoplasmic reticulum adaptor that facilitates innate immune signalling. *Nature* **455**, 674–678 (2008).

16. Sun, L., Wu, J., Du, F., Chen, X. & Chen, Z. J. Cyclic GMP-AMP Synthase Is a Cytosolic DNA Sensor That Activates the Type I Interferon Pathway. *Science* **339**, 786–791 (2013).

17. Burdette, D. L. *et al.* STING is a direct innate immune sensor of cyclic di-GMP. *Nature* **478**, 515–518 (2011).

18. Diner, E. J. *et al.* The Innate Immune DNA Sensor cGAS Produces a Noncanonical Cyclic Dinucleotide that Activates Human STING. *Cell Reports* **3**, 1355–1361 (2013).

19. Gao, P. *et al.* Cyclic [G(2′,5′)pA(3′,5′)p] Is the Metazoan Second Messenger Produced by DNA-Activated Cyclic GMP-AMP Synthase. *Cell* **153**, 1094–1107 (2013).

20. Ablasser, A. *et al.* cGAS produces a 2′-5′-linked cyclic dinucleotide second messenger that activates STING. *Nature* **498**, 380–384 (2013).

21. Moretti, J. *et al.* STING Senses Microbial Viability to Orchestrate Stress-Mediated Autophagy of the Endoplasmic Reticulum. *Cell* **171**, 809-823.e13 (2017).

22. Cohen, D. *et al.* Cyclic GMP–AMP signalling protects bacteria against viral infection. *Nature* **574**, 691–695 (2019).

23. Morehouse, B. R. *et al.* STING cyclic dinucleotide sensing originated in bacteria. *Nature* 1–8 (2020) doi:10.1038/s41586-020-2719-5.

24. Burroughs, A. M. & Aravind, L. Identification of Uncharacterized Components of Prokaryotic Immune Systems and Their Diverse Eukaryotic Reformulations. *J Bacteriol* **202**, (2020).

25. Alegado, R. A. *et al.* A bacterial sulfonolipid triggers multicellular development in the closest living relatives of animals. *Elife* **1**, e00013 (2012).

26. Brunet, T. *et al.* A flagellate-to-amoeboid switch in the closest living relatives of animals. *Elife* **10**, e61037 (2021).

27. Dayel, M. J. *et al.* Cell differentiation and morphogenesis in the colony-forming choanoflagellate Salpingoeca rosetta. *Dev Biol* **357**, 73 82 (2011).

28. Woznica, A., Gerdt, J. P., Hulett, R. E., Clardy, J. & King, N. Mating in the Closest Living Relatives of Animals Is Induced by a Bacterial Chondroitinase. *Cell* **170**, 1175 1183.e11 (2017).

29. Brunet, T. *et al.* Light-regulated collective contractility in a multicellular choanoflagellate. *Science* **366**, 326–334 (2019).

30. Laundon, D., Larson, B. T., McDonald, K., King, N. & Burkhardt, P. The architecture of cell differentiation in choanoflagellates and sponge choanocytes. *Plos Biol* **17**, e3000226 (2019).

31. Woznica, A. *et al.* Bacterial lipids activate, synergize, and inhibit a developmental switch in choanoflagellates. *Proc National Acad Sci* **113**, 7894 7899 (2016).

32. Ireland, E. V., Woznica, A. & King, N. Synergistic Cues from Diverse Bacteria Enhance Multicellular Development in a Choanoflagellate. *Appl Environ Microb* **86**, (2020).

33. Hake, K. *et al.* Colonial choanoflagellate isolated from Mono Lake harbors a microbiome. doi:10.1101/2021.03.30.437421.

34. Moradali, M. F., Ghods, S. & Rehm, B. H. A. Pseudomonas aeruginosa Lifestyle: A Paradigm for Adaptation, Survival, and Persistence. *Front Cell Infect Mi* **7**, 39 (2017).

35. Mahajan-Miklos, S., Tan, M.-W., Rahme, L. G. & Ausubel, F. M. Molecular Mechanisms of Bacterial Virulence Elucidated Using a Pseudomonas aeruginosa– Caenorhabditis elegans Pathogenesis Model. *Cell* **96**, 47–56 (1999).

36. Pukatzki, S., Kessin, R. H. & Mekalanos, J. J. The human pathogen Pseudomonas aeruginosa utilizes conserved virulence pathways to infect the social amoeba Dictyostelium discoideum. *Proc National Acad Sci* **99**, 3159–3164 (2002).

37. Rahme, L. G. *et al.* Use of model plant hosts to identify Pseudomonas aeruginosa virulence factors. *Proc National Acad Sci* **94**, 13245–13250 (1997).

38. Uribe-Querol, E. & Rosales, C. Control of Phagocytosis by Microbial Pathogens. *Front Immunol* **8**, 1368 (2017).

39. Yoon, S. *et al.* Pseudomonas syringae evades phagocytosis by animal cells via type III effector-mediated regulation of actin filament plasticity. *Environ Microbiol* **20**, 3980–3991 (2018).

40. Klockgether, J. & Tümmler, B. Recent advances in understanding Pseudomonas aeruginosa as a pathogen. *F1000research* **6**, 1261 (2017).

41. Tanaka, Y. & Chen, Z. J. STING Specifies IRF3 Phosphorylation by TBK1 in the Cytosolic DNA Signaling Pathway. *Sci Signal* **5**, ra20–ra20 (2012).

42. Liu, S. *et al.* Phosphorylation of innate immune adaptor proteins MAVS, STING, and TRIF induces IRF3 activation. *Science* **347**, aaa2630 (2015).

43. Zhang, C. *et al.* Structural basis of STING binding with and phosphorylation by TBK1. *Nature* **567**, 394–398 (2019).

44. Abe, T. & Barber, G. N. Cytosolic-DNA-Mediated, STING-Dependent Proinflammatory Gene Induction Necessitates Canonical NF-κB Activation through TBK1. *J Virol* **88**, 5328–5341 (2014).

45. Gui, X. *et al.* Autophagy induction via STING trafficking is a primordial function of the cGAS pathway. *Nature* **567**, 262–266 (2019).

46. Yamashiro, L. H. *et al.* Interferon-independent STING signaling promotes resistance to HSV-1 in vivo. *Nat Commun* **11**, 3382 (2020).

47. Prabakaran, T. *et al.* Attenuation of cGAS-STING signaling is mediated by a p62/SQSTM1-dependent autophagy pathway activated by TBK1. *Embo J* **37**, (2018).

48. Mann, C. C. de O. *et al.* Modular Architecture of the STING C-Terminal Tail Allows Interferon and NF-κB Signaling Adaptation. *Cell Reports* **27**, 1165-1175.e5 (2019).

49. Watson, R. O. *et al.* The Cytosolic Sensor cGAS Detects Mycobacterium tuberculosis DNA to Induce Type I Interferons and Activate Autophagy. *Cell Host Microbe* **17**, 811–819 (2015).

50. Booth, D. S., Szmidt-Middleton, H. & King, N. Choanoflagellate transfection illuminates their cell biology and the ancestry of animal septins. *Mol Biol Cell* **29**, mbcE18080514 (2018).

51. Dobbs, N. *et al.* STING Activation by Translocation from the ER Is Associated with Infection and Autoinflammatory Disease. *Cell Host Microbe* **18**, 157–168 (2015).

52. Booth, D. S. & King, N. Genome editing enables reverse genetics of multicellular development in the choanoflagellate Salpingoeca rosetta. *Elife* **9**, e56193 (2020).

53. Liu, Y. *et al.* Inflammation-Induced, STING-Dependent Autophagy Restricts Zika Virus Infection in the Drosophila Brain. *Cell Host Microbe* **24**, 57-68.e3 (2018).

54. Klionsky, D. J. *et al.* Guidelines for the use and interpretation of assays for monitoring autophagy (4th edition) 1. *Autophagy* **17**, 1–382 (2021).

55. Tanida, I., Minematsu-Ikeguchi, N., Ueno, T. & Kominami, E. Lysosomal Turnover, but Not a Cellular Level, of Endogenous LC3 is a Marker for Autophagy. *Autophagy* **1**, 84–91 (2005).

56. Pokatayev, V. *et al.* Homeostatic regulation of STING protein at the resting state by stabilizer TOLLIP. *Nat Immunol* **21**, 158–167 (2020).

57. McFarland, A. P. *et al.* Sensing of Bacterial Cyclic Dinucleotides by the Oxidoreductase RECON Promotes NF-κB Activation and Shapes a Proinflammatory Antibacterial State. *Immunity* **46**, 433–445 (2017).

58. Margolis, S. R. *et al.* The STING ligand 2′3′-cGAMP induces an NF-κB-dependent anti-bacterial innate immune response in the starlet sea anemone Nematostella vectensis. (2021) doi:10.1101/2021.05.13.443009.

59. Cai, H. *et al.* 2′3′-cGAMP triggers a STING- and NF-κB–dependent broad antiviral response in Drosophila. *Sci Signal* **13**, eabc4537 (2020).

60. Martin, M., Hiroyasu, A., Guzman, R. M., Roberts, S. A. & Goodman, A. G. Analysis of Drosophila STING Reveals an Evolutionarily Conserved Antimicrobial Function. *Cell Reports* **23**, 3537-3550.e6 (2018).

61. Goto, A. *et al.* The Kinase IKKβ Regulates a STING- and NF-κB-Dependent Antiviral Response Pathway in Drosophila. *Immunity* **49**, 225-234.e4 (2018).

62. Hua, X. *et al.* Stimulator of interferon genes (STING) provides insect antiviral immunity by promoting Dredd caspase–mediated NF-κB activation. *J Biol Chem* **293**, 11878–11890 (2018).

63. Schindelin, J. *et al.* Fiji: an open-source platform for biological-image analysis. *Nat Methods* **9**, 676–682 (2012).

64. Kim, D. *et al.* TopHat2: accurate alignment of transcriptomes in the presence of insertions, deletions and gene fusions. *Genome Biol* **14**, R36 (2013).

65. Liao, Y., Smyth, G. K. & Shi, W. featureCounts: an efficient general purpose program for assigning sequence reads to genomic features. *Bioinformatics* **30**, 923–930 (2014).

66. Robinson, M. D., McCarthy, D. J. & Smyth, G. K. edgeR: a Bioconductor package for differential expression analysis of digital gene expression data. *Bioinformatics* **26**, 139–140 (2010).

67. Peng, D., Kurup, S. P., Yao, P. Y., Minning, T. A. & Tarleton, R. L. CRISPR-Cas9-Mediated Single-Gene and Gene Family Disruption in Trypanosoma cruzi. *Mbio* **6**, e02097-14 (2015).

**Table 1. Bacteria screened for pathogenic effects**

| Bacterium | Pathogenic effects | Reference or details | Source |
|---|---|---|---|
| *Aeromonas hyrophila* | – | Environmental isolate | This study |
| *Bacillus aquimaris* | – | Environmental isolate | This study |
| *Bacillus badius* | – | Mouse isolate | Julie Pfeiffer |
| *Bacillus cereus* | – | Environmental isolate | This study |
| *Bacillus indicus* | – | Environmental isolate | This study |
| *Bacillus marisflavi* | – | Environmental isolate | This study |
| *Bacillus pumilus* | – | Mouse isolate | Julie Pfeiffer |
| *Bacillus safensis* | – | Mouse isolate | Julie Pfeiffer |
| *Bacillus subtilus* | – | ATCC 6633 | Julie Pfeiffer |
| *Bacteroides acidifaciens* | – | Mouse isolate | Julie Pfeiffer |
| *Burkholderia multivorans* | – | ATCC 17616 | David Greenberg |
| *Campylobacter jejuni* GFP | – | DRH3123 | David Hendrixson |
| *Deinococcus* sp. | – | Environmental isolate | This study |
| *Enterococcus cloacae* | – | Mouse isolate | Julie Pfeiffer |
| *Enterococcus faecium* | – | Mouse isolate | Julie Pfeiffer |
| *Escherichia coli* BW25113 | – | Datsenko and Wanner, 2000 | David Greenberg |
| *Escherichia coli DH5a* GFP | – | | David Hendrixson |
| *Escherichia coli* ECC-1470 | – | Leimbach et al., 2015 | Julie Pfeiffer |
| *Escherichia coli* K12 | – | ATCC 10798 | Julie Pfeiffer |
| *Flavobacterium sp.* | – | King et al., 2008 | Isolated from ATCC PRA-258 |
| *Lactobacillus johnsonii* | – | Mouse isolate | Julie Pfeiffer |
| *Pseudoalteromonas sp.* | – | Environmental isolate | This study |
| *Pseudomonas aeruginosa* PA-14 | + | Rahm et al., 1995 | Andrew Koh |
| *Pseudomonas aeruginosa* PAO1 | + | ATCC 15692 | David Greenberg |
| *Pseudomonas aeruginosa* PAO1-GFP | + | Bloemberg et al., 1997 | David Greenberg |
| *Pseudomonas granadensis* | – | Environmental isolate | This study |
| *Staphylococcus aureus* | – | ATCC 23235 | Julie Pfeiffer |
| *Staphylococcus* sp. | – | Mouse isolate | Julie Pfeiffer |
| *Vibrio alginolyticus* | – | Environmental isolate | Kim Orth |
| *Vibrio furnissii* | – | Environmental isolate | This study |
| *Vibrio parahaemolyticus* | – | Environmental isolate | This study |
| *Vibrio parahaemolyticus* RimD-GFP | – | Ritchie et al., 2012 | Kim Orth |
| *Vibrio ruber* | – | Environmental isolate | This study |
| *Vibrio sp.* | – | Environmental isolate | This study |

**Table 2. *P. aeruginosa* deletion strains**

| Strain name | Gene | Putative ORF function | Effects on *M. brevicollis* | |
|---|---|---|---|---|
| | | | Truncated Flagellum/ Settling | Cell Death |
| MPAO1 | | parent to library stain | + | + |
| PW5035 | pvdE | pyoverdine biosynthesis protein PvdE | + | + |
| PW5034 | pvdE | pyoverdine biosynthesis protein PvdE | + | + |
| PW1059 | exoT | exoenzyme T | + | + |
| PW3078 | toxA | exotoxin A precursor | + | + |
| PW3079 | toxA | exotoxin A precursor | + | + |
| PW4736 | exoY | adenylate cyclase ExoY | + | + |
| PW4737 | exoY | adenylate cyclase ExoY | + | + |
| PW6886 | rhlA | rhamnosyltransferase chain A | + | + |
| PW6887 | rhlA | rhamnosyltransferase chain A | + | + |
| PW7478 | exoS | exoenzyme S | + | + |
| PW7479 | exoS | exoenzyme S | + | + |
| PW7303 | lasB | elastase LasB | + | + |
| PW7302 | lasB | elastase LasB | + | + |
| PW3252 | aprA | alkaline metalloproteinase precursor | + | + |
| PW3253 | aprA | alkaline metalloproteinase precursor | + | + |
| PW4282 | lasA | LasA protease precursor | + | + |
| PW4283 | lasA | LasA protease precursor | + | + |
| RP436 | popB | T3SS translocase | + | + |
| RP576 | exoS, exoT, exoY | T3SS effector molecules | + | + |

**Table 3. *M. brevicollis* response to *P. aeruginosa* factors**

| Treatment | Cell Death | Interpretation |
|---|---|---|
| Live *P. aeruginosa* | ++ | |
| *P. aeruginosa* conditioned media (CM) | ++ | Factor(s) are secreted by *P. aeruginosa* |
| *P. aeruginosa* outer membrane vesicles | – | Factor(s) are not present in outer membrane vesicles |
| CM, boiled 20 min | ++ | Factor(s) are not heat labile |
| CM + proteinase K, followed by 80C for 30 min | ++ | Factor(s) are not proteins |
| CM + DNAse and RNAse | ++ | Factor(s) are not nucleic acids |
| CM MeOH extraction | ++ | Factor(s) are organic compounds |

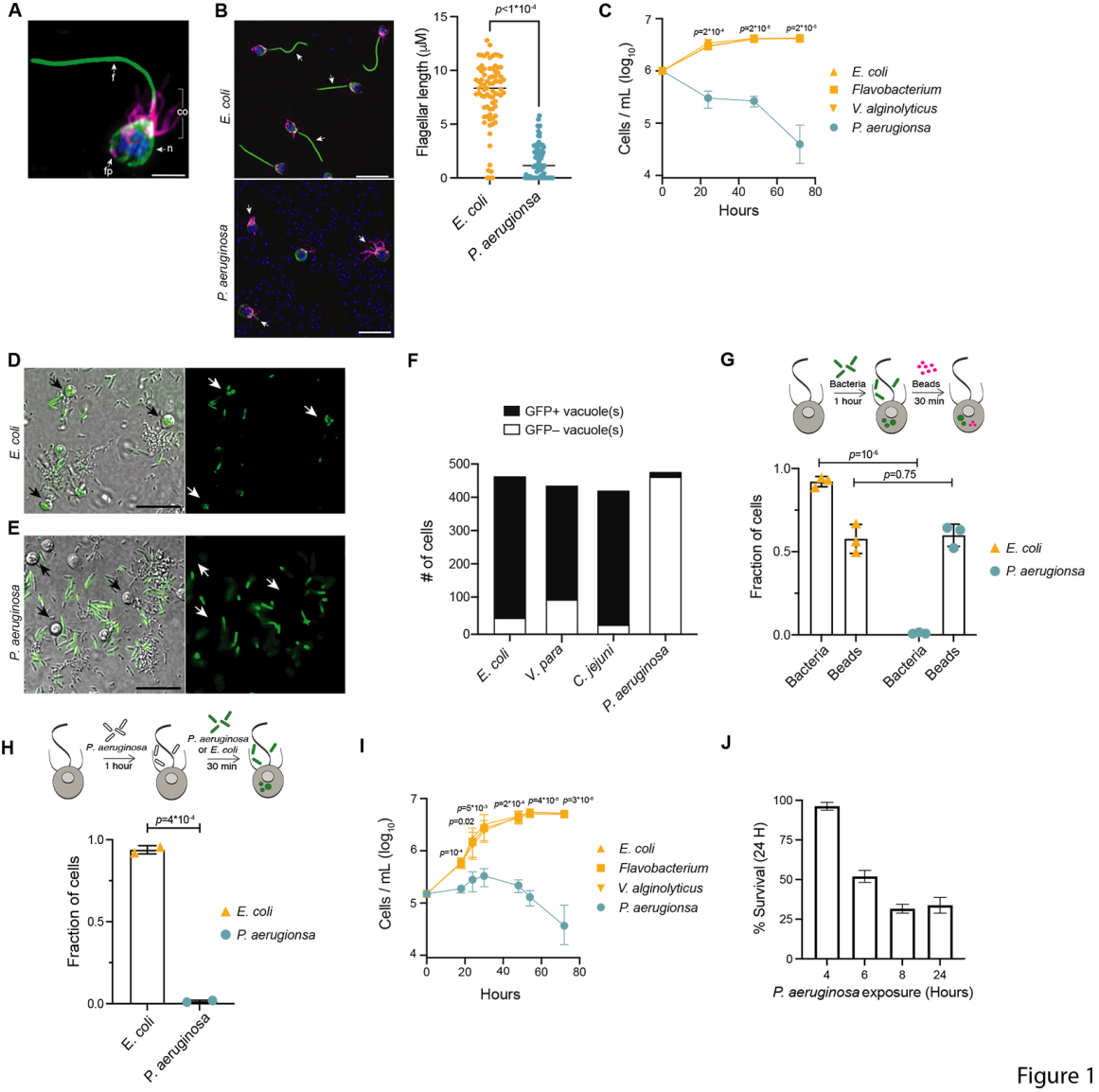
A
f
co
n
fp
B
E. coli
P. aeruginosa
p<1*10-4
Flagellar length (μM)
E. coli
P. aeruginosa
C
p=2*10-4
p=2*10-6
p=2*10-5
Cells / mL (log10)
Hours
E. coli
Flavobacterium
V. alginolyticus
P. aeruginosa
D
E. coli
E
P. aeruginosa
F
GFP+ vacuole(s)
GFP– vacuole(s)
# of cells
E. coli
V. para
C. jejuni
P. aeruginosa
G
Bacteria
1 hour
Beads
30 min
p=10-6
p=0.75
Fraction of cells
Bacteria
Beads
Bacteria
Beads
E. coli
P. aeruginosa
H
P. aeruginosa
1 hour
P. aeruginosa
or E. coli
30 min
p=4*10-4
Fraction of cells
E. coli
P. aeruginosa
I
p=5*10-3
p=2*10-4
p=4*10-5
p=3*10-6
p=0.02
p=10-4
Cells / mL (log10)
Hours
E. coli
Flavobacterium
V. alginolyticus
P. aeruginosa
J
% Survival (24 H)
P. aeruginosa exposure (Hours)

Figure 1

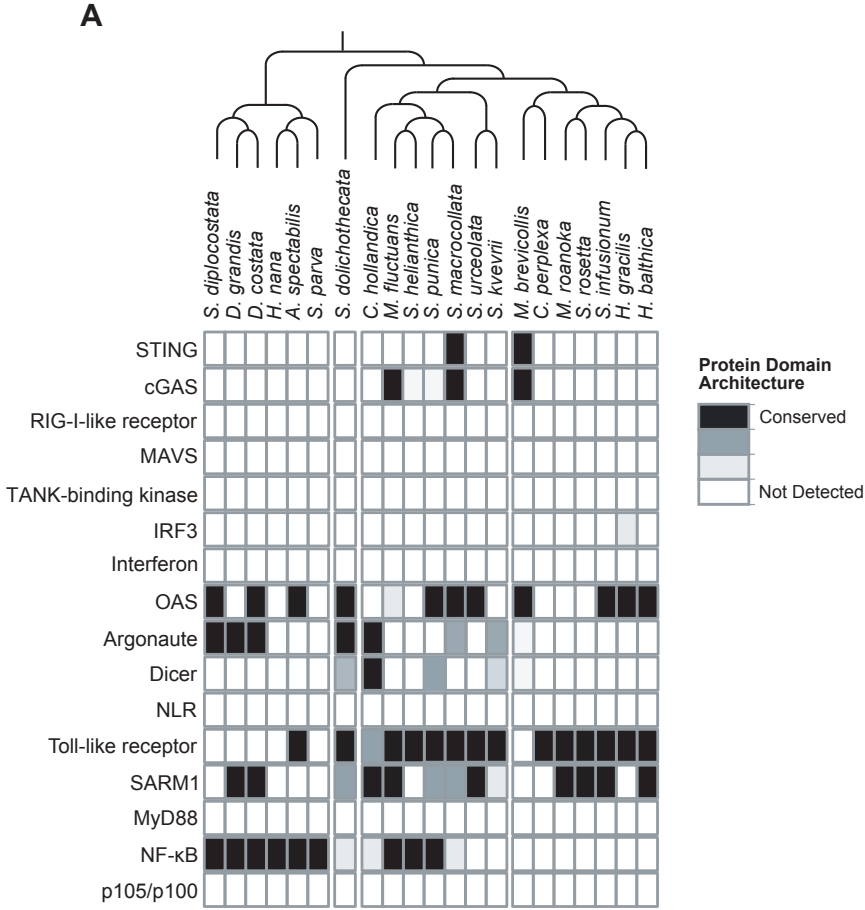


Figure 1 - figure supplement 1

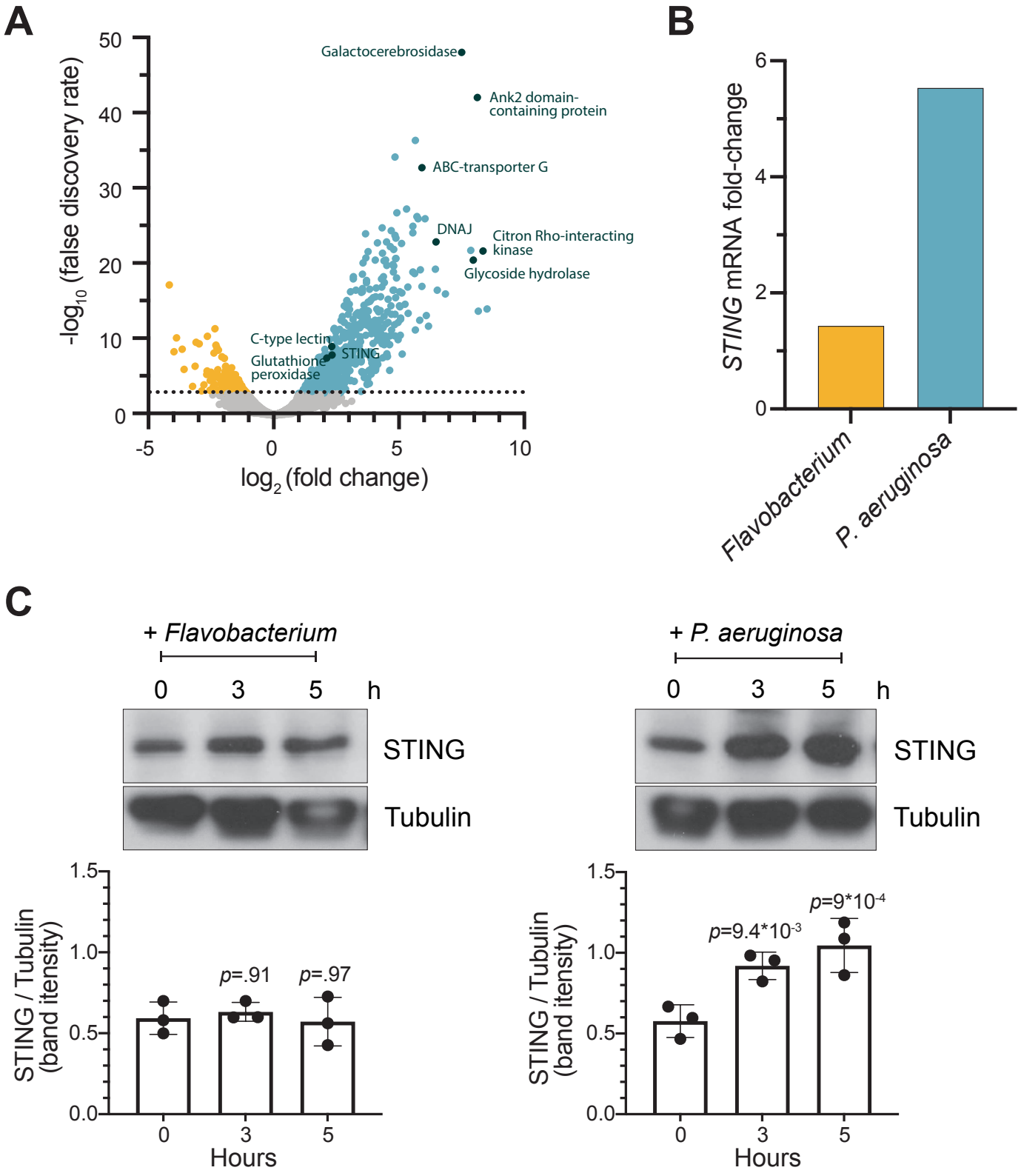
A
Galactocerebrosidase
Ank2 domain-containing protein
ABC-transporter G
DNAJ
Citron Rho-interacting kinase
Glycoside hydrolase
C-type lectin
STING
Glutathione peroxidase
-log10 (false discovery rate)
log2 (fold change)
B
STING mRNA fold-change
Flavobacterium
P. aeruginosa
C
+ Flavobacterium
0 3 5 h
STING
Tubulin
STING / Tubulin (band itensity)
p=.91
p=.97
Hours
+ P. aeruginosa
0 3 5 h
STING
Tubulin
STING / Tubulin (band itensity)
p=9.4*10-3
p=9*10-4
Hours

Figure 2

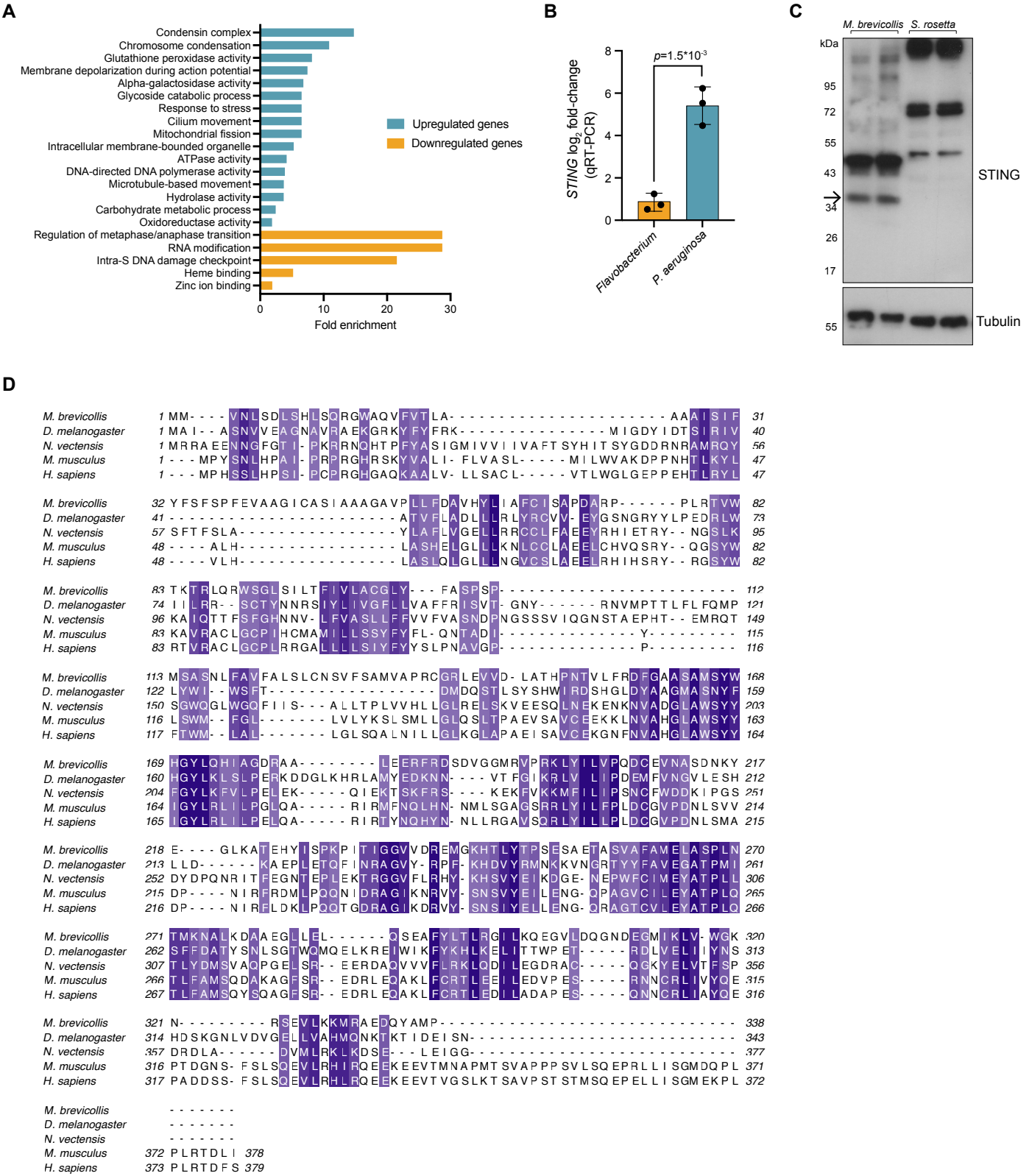


Figure 2 - figure supplement 1

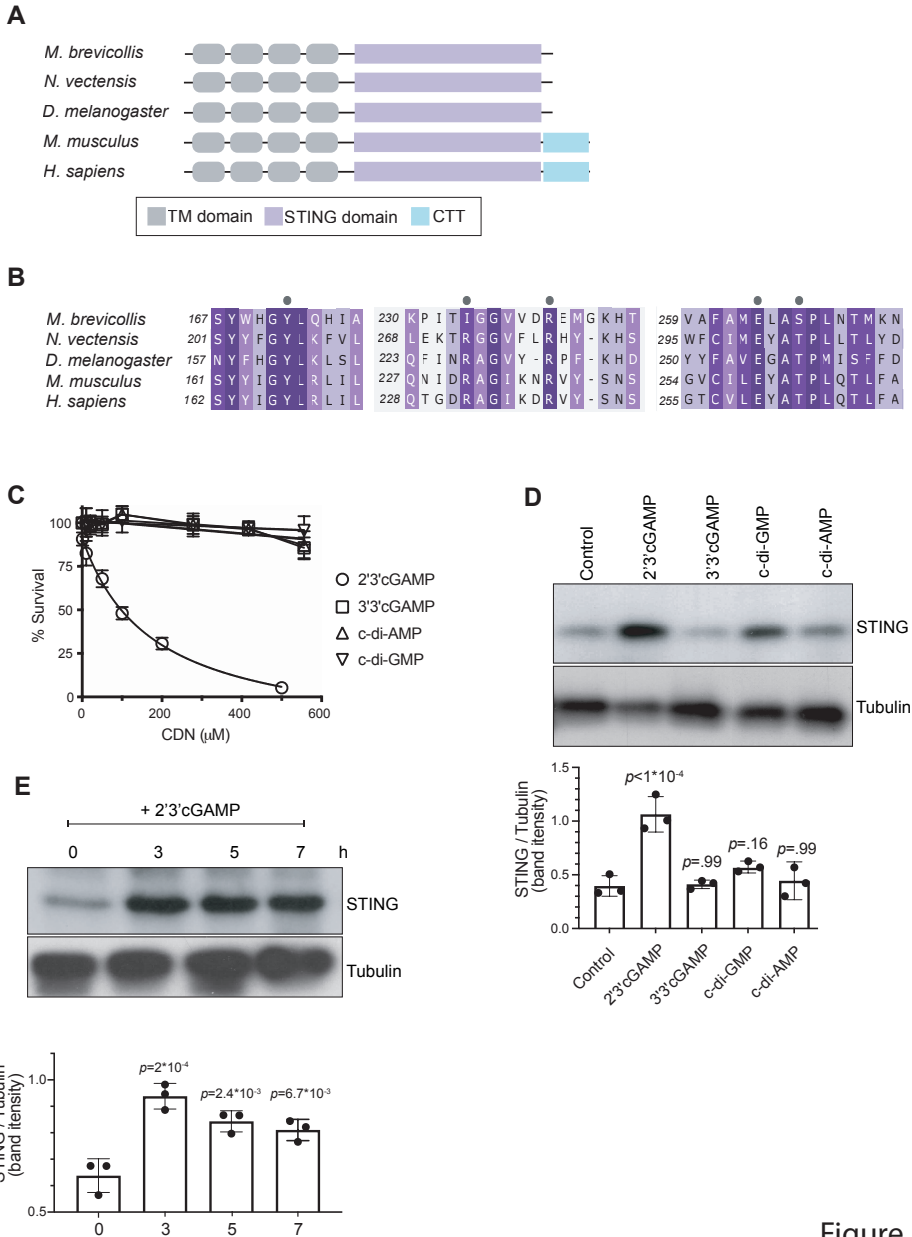
A
M. brevicollis
N. vectensis
D. melanogaster
M. musculus
H. sapiens
TM domain
STING domain
CTT
B
M. brevicollis 167 SYWHGYLQHIA 230 KPITIGGVVDREMGKHT 259 VAFAMELASPLNTMKN
N. vectensis 201 SYYFGYLKFVL 268 LEKTRGGVFLRHY-KHS 295 WFCIMEYATPLLTLYD
D. melanogaster 157 NYFHGYLKLSL 223 QFINRAGVY-RPF-KHD 250 YYFAVEGATPMISFFD
M. musculus 161 SYYIGYLRLIL 227 QNIDRAGIKNRVY-SNS 254 GVCILEYATPLQTLFA
H. sapiens 162 SYYIGYLRLIL 228 QTGDRAGIKDRVY-SNS 255 GTCVLEYATPLQTLFA
C
% Survival
CDN (μM)
2'3'cGAMP
3'3'cGAMP
c-di-AMP
c-di-GMP
D
Control
2'3'cGAMP
3'3'cGAMP
c-di-GMP
c-di-AMP
STING
Tubulin
STING / Tubulin (band itensity)
p<1*10-4
p=.99
p=.16
p=.99
E
+ 2'3'cGAMP
0 3 5 7 h
STING
Tubulin
STING / Tubulin (band itensity)
p=2*10-4
p=2.4*10-3
p=6.7*10-3

Figure 3

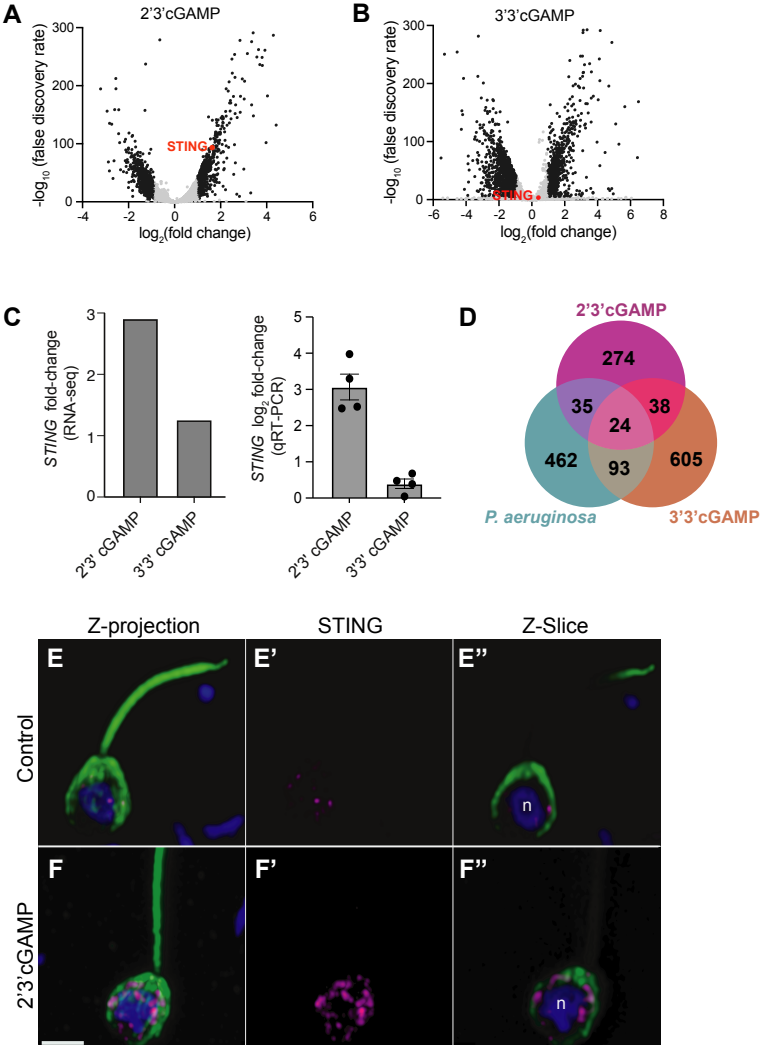


Figure 3 - figure supplement 1

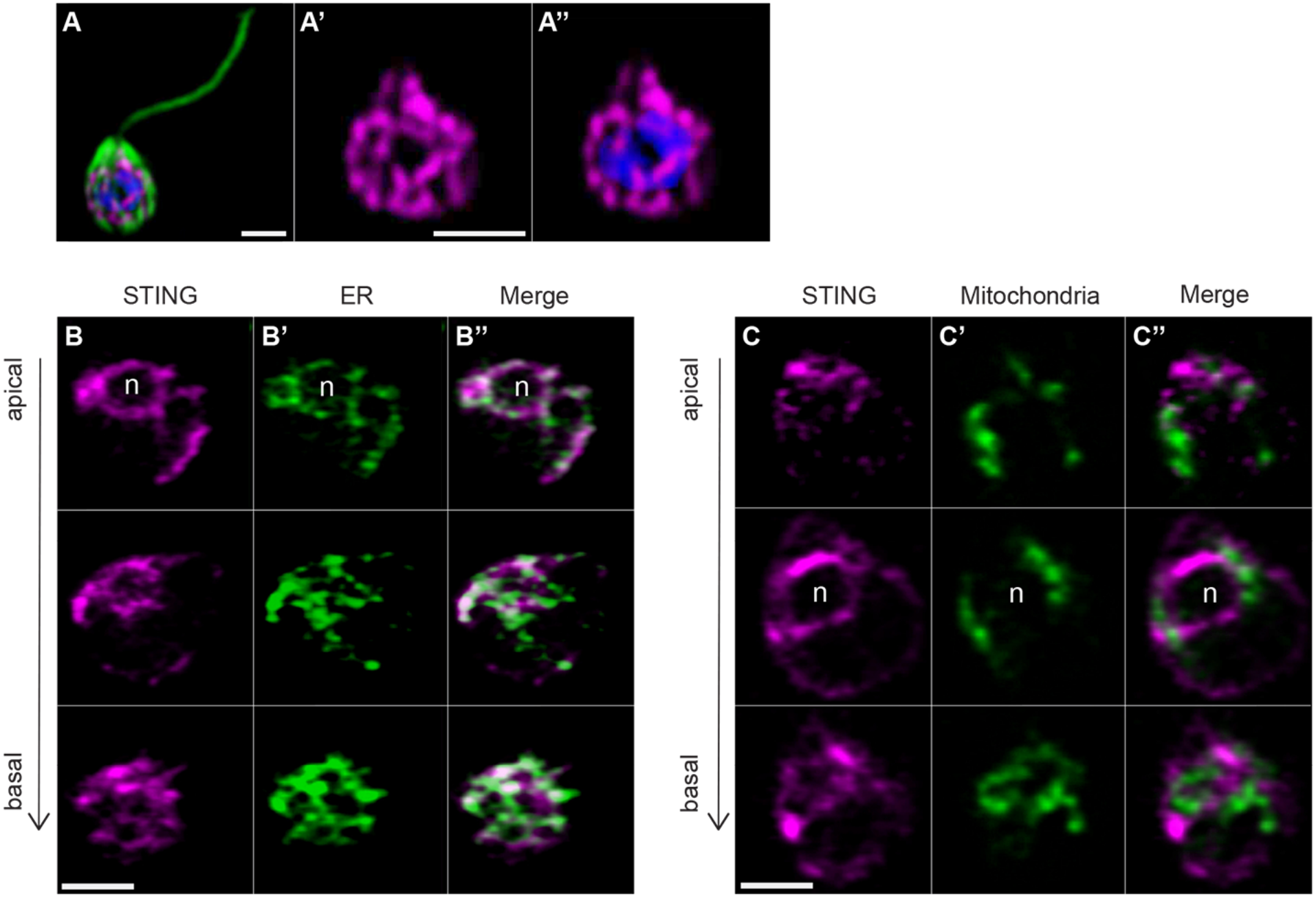
A
A'
A''
STING
ER
Merge
B
B'
B''
n
apical
basal
STING
Mitochondria
Merge
C
C'
C''
n
apical
basal

Figure 4

**A**

| Strain | *STING* locus (sc5:1254441) |
|---|---|
| Wild Type | TTCAGATGTGGGCGGCATGCGAGTT |
| *STING*⁻ | TTCAGATG----------CATGCGAGTT |

**B**

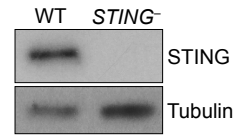


**C**

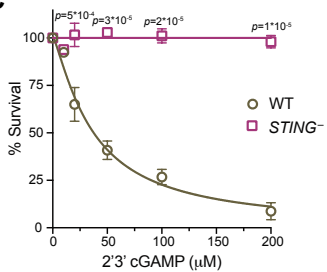


**D**

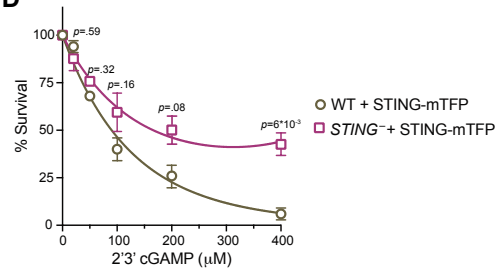


**E**

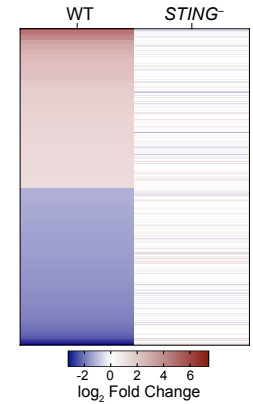


**F**

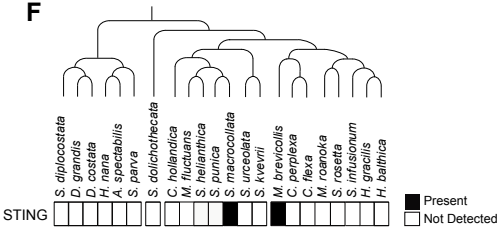


**G**

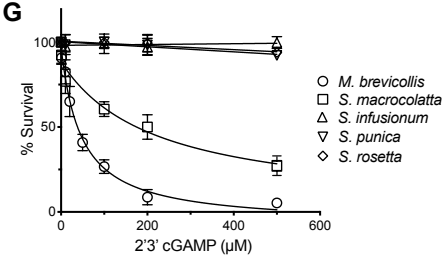


**H**

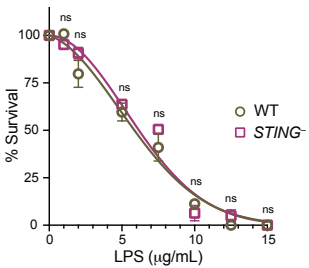


**I**

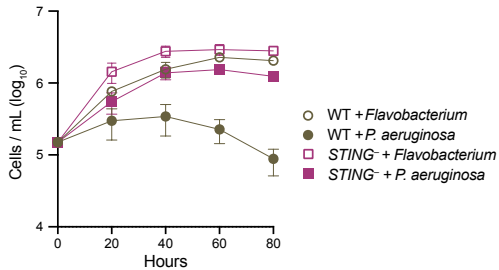


**J**

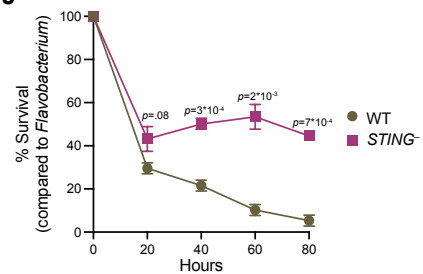


Figure 5

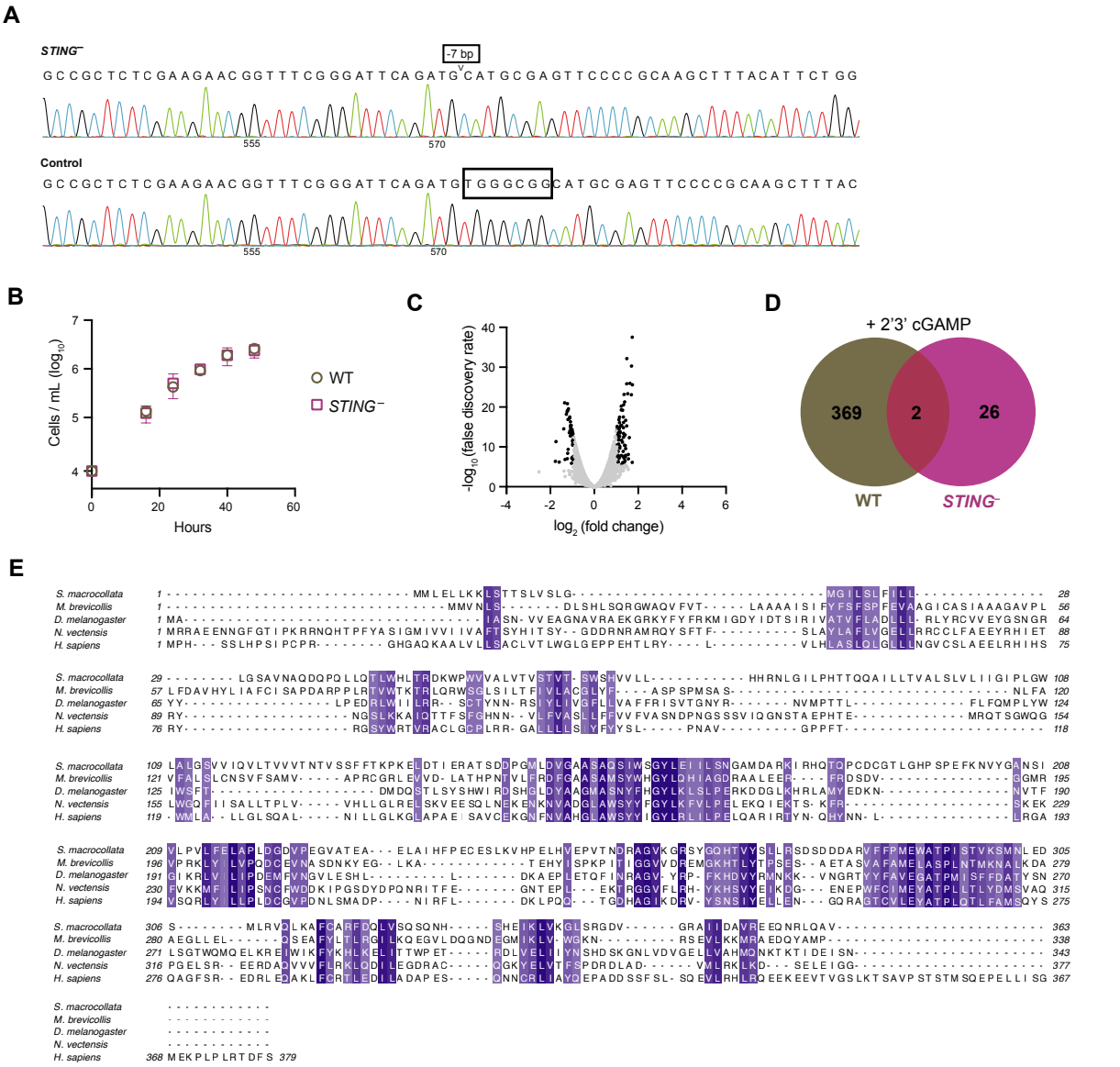


Figure 5 - figure supplement 1

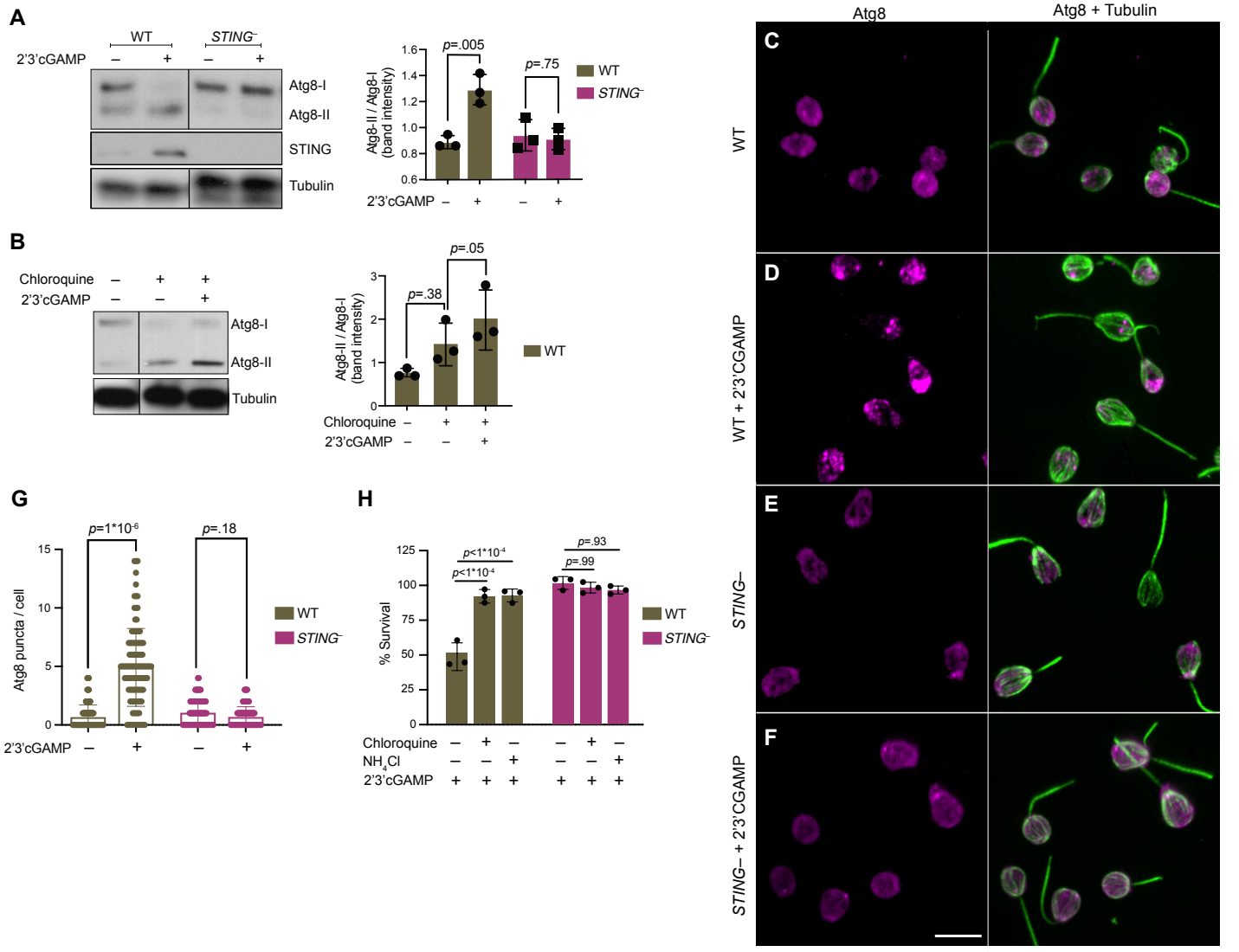
A
WT
STING⁻
2'3'cGAMP
Atg8-I
Atg8-II
STING
Tubulin
Atg8-II / Atg8-I (band intensity)
p=.005
p=.75
WT
STING⁻
B
Chloroquine
2'3'cGAMP
Atg8-I
Atg8-II
Tubulin
Atg8-II / Atg8-I (band intensity)
p=.38
p=.05
WT
G
Atg8 puncta / cell
p=1*10-6
p=.18
WT
STING⁻
H
% Survival
p<1*10-4
p<1*10-4
p=.93
p=.99
WT
STING⁻
Chloroquine
NH4Cl
2'3'cGAMP
Atg8
Atg8 + Tubulin
C
D
E
F
WT
WT + 2'3'CGAMP
STING–
STING– + 2'3'CGAMP

Figure 6

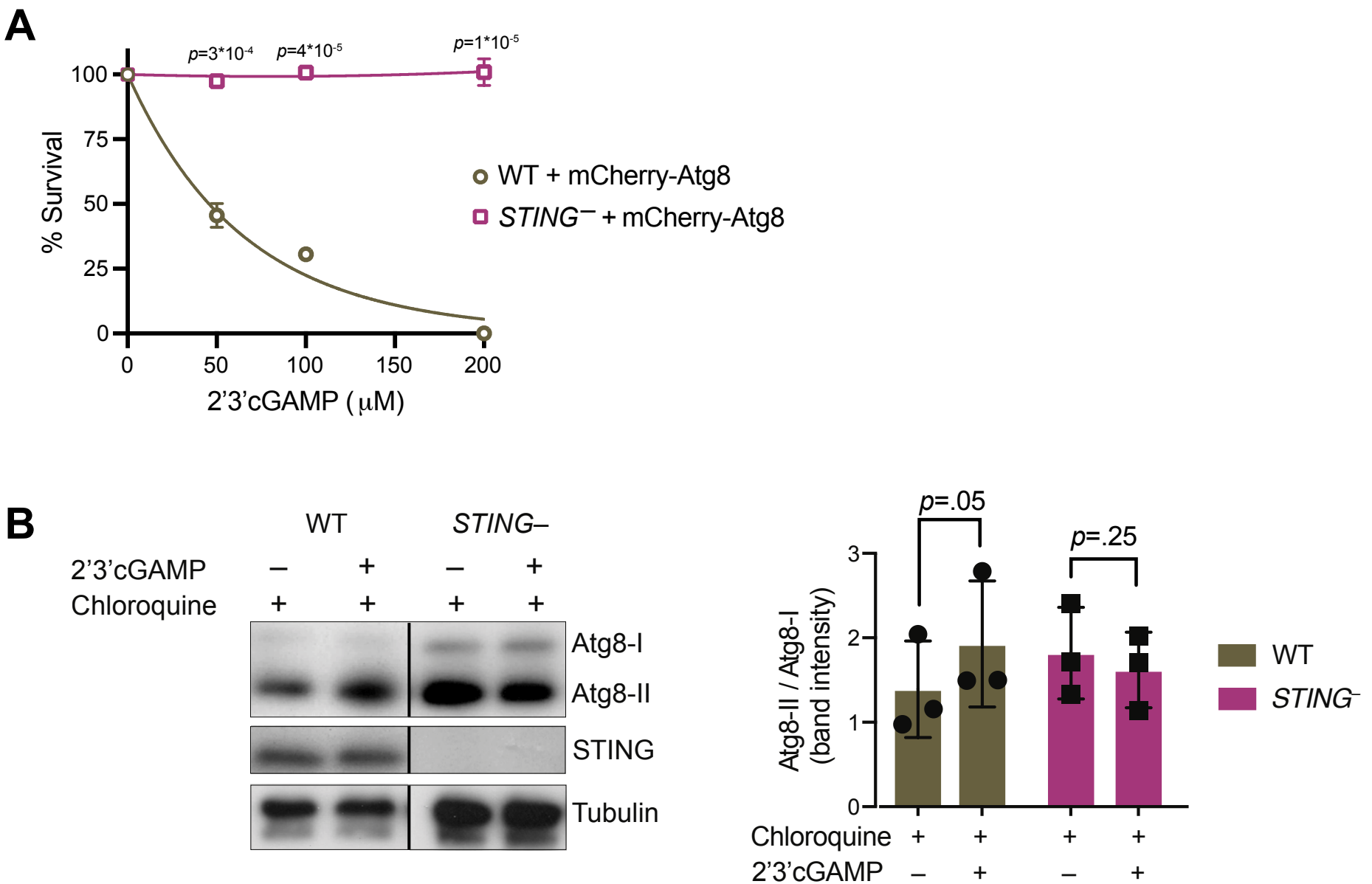


Figure 6 - figure supplement 1